Interuniversity Master's Degree in Nuclear Physics

Master Thesis

$\Sigma\Sigma \to YN$ transitions
in the decay of $^{6}_{\Lambda\Lambda}\text{He}$

Ariadna Aixut López

Superviors: Assumpta Parreño García (UB)
Laura Tolós Rigueiro (ITP, FIAS, ICE)
Universitat de Barcelona
Quantum Physics and Astrophysics Department
December 2019

"If a theory is complicated, its wrong"

Richard Feynman

Acknowledgments

Aquest treball ha representat per a mi un abans i un després en la meva manera de veure la física. I és que la recerca no es tanca mai definitivament, sinó que sempre hi haurà una nova manera d'enfocar una recerca i nous càlculs per a desenvolupar o afinar.

M'agradaria agraïr a les dues meves tutores, l'Assumpta i la Laura, tot l'esforç i dedicació que han volcat en aquest treball. Sense elles, no hagúes estat possible. M'agradaria agraïr a l'Assumpta, en especial, tots els moments en que ha estat més que una tutora i m'ha recolzat, cuidat i esperonat quan més ho necessitava, des que ens vam conèixer quan jo només era al tercer any del grau. Gràcies a les dues de tot cor.

És obligatori agrair també al Jordi Maneu tota la feina feta per al meu treball, tant davant d'un teclat com d'un full en blanc.

Sense menys importància, gràcies a l'Anna per recolzar-me i ajudar-me en aquest treball, i en tot el camí que hem fet juntes fins aquí.

Com sempre, no pot faltar una menció als meus pares, l'Ernest i la Rosa, sense els quals no hagúes arribat mai on sóc.

Contents

I. Introduction

A hypernucleus is a bound system of nucleons and at least one hyperon, where hyperons are baryons containing strange quarks. The presence of the strange quark makes hyperons spaecially attractive to study since these systems are unstable with respect to the weak force, leading to the appearance of weak decays which do not conserve neither parity, isospin nor flavour.

Traditionally, the study of the decay of single-Λ hypernuclei has captured most of the attention [1][2][3] , since they are the lightest strange bound systems and consequently the easiest to produce. Hypernuclei are usually produced with hadronic reactions in excited states. To reach the ground state, these nuclei typically experiment a deexcitation process which often includes the emission of particles or electromagnetic radiation. Once in the ground state, these nuclei decay through weak interaction processes, as the ones studied in the present work.

A Λ hyperon in free space decays weakly, with a lifetime of $\tau_\Lambda = (2.631 \pm 0.020) \times 10^{-10}$ s, leading to nucleons and pions (mesonic decay mode) in the final state with an approximate ratio $\Gamma(\Lambda \to p\pi^-)/\Gamma(\Lambda \to n\pi^0) \sim 2$, which is compatible with a change in isospin along the decay process of $\Delta I = 1/2$. The observed suppression of $\Delta I = 3/2$ transitions over $\Delta I = 1/2$ ones has motivated a number of theoretical investigations, as that of Ref. [4], but a fundamental understanding of its origin is still missing. When the hyperon is bound in the nuclear medium this decay mode is Pauli blocked, since the emerging nucleon tries to access momentum states that are already occupied by the surrounding nucleons, and non-mesonic decay modes induced by the presence of these nucleons ($\Lambda N \to NN$) become dominant.

Recently, the attention has been focused on doubly strange systems which offer a richer scenario that includes additional decay channels. In the present work we study the decay of $^{6}_{\Lambda\Lambda}$He. This hypernucleus was first observed in the KEK-E373 experiment [5], which aroused great interest on theoretical and experimental studies involving the $\Lambda\Lambda$ interaction. Since then, other $\Lambda\Lambda$-hypernuclei have been observed, allowing for a precise extraction of the $\Lambda\Lambda$ binding energy, as well as many other nuclear properties. More recently, the E07 experiment at J-PARC [6, 7] aims to produce $\Lambda\Lambda$ nuclei throughout the capture of Ξ hyperons, with the subsequent strong conversion into $\Lambda\Lambda$ pairs. It is estimated that the statistical sample will be an order of magnitude greater than the one in experiment KEK-E373, allowing for a more accurate extraction of the strong and weak baryon-baryon (BB) interaction observables in the strange sector.

Due to the strong interaction acting on the baryons, the ΛN and $\Lambda\Lambda$ pairs in the initial hypernucleus can mix with other baryon-baryon (BB) channels with either one-unit or two-units of strangeness, ΣN and ΞN and $\Sigma\Sigma$ respectively. The different components of the wave functions are contained in the solution of the G-matrix equations. These initial two-body particle states will in turn decay via weak processes leading to BB states which leave the system with enough momenta to be treated with a T-matrix formalism, where no medium corrections are considered.

In Ref. [8] the decay of $^{6}_{\Lambda\Lambda}$He induced by $\Lambda N \rightarrow NN$ and $\Lambda\Lambda \rightarrow \Lambda N(\Sigma N)$ transitions was studied. In this work, the decay rates to the different final states were calculated to be: $\Gamma_{NN} = 0.96\Gamma_{\Lambda}$, $\Gamma_{\Lambda N} = 3.58 \times 10^{-2}\Gamma_{\Lambda}$ and $\Gamma_{\Sigma N} = 3.0 \times 10^{-3}\Gamma_{\Lambda}$, where $\Gamma_{\Lambda} = 3.8 \times 10^{9}s^{-1}$ corresponds to the decay rate of a Λ in free space. The total contribution added up to a final value for the rate of $\Gamma = 0.96\Gamma_{\Lambda}$, dominated by the exchange of π and the K mesons in the weak model.

As it can be seen from Fig. 1 (taken from Ref. [9]), the dominant component of the $\Lambda\Lambda$ wave function is the diagonal $\Lambda\Lambda - \Lambda\Lambda$ one, with the $\Lambda\Lambda - \Xi N$ being the quantitatively second in importance in the relevant region. This fact motivated the work of Refs. [9, 10], with the inclusion of the $\Xi N \rightarrow YN$ decay channel in the formalism, which modified the results presented in [8]. While the ΛN contribution experimented a decrease, giving a value of $\Gamma_{\Lambda N} = 1.31 \times 10^{-2}\Gamma_{\Lambda}$, the ΣN contribution increased its value to $\Gamma_{\Sigma N} = 2.67 \times 10^{-2}\Gamma_{\Lambda}$, adding to a total contribution of $\Gamma = 3.98 \times 10^{-2}\Gamma_{\Lambda}$. Nevertheless, a complete study of the decay process must include all the components of the wave function. The remaining contribution is the one coming from the $\Lambda\Lambda - \Sigma\Sigma$ channel, for which one expects an even smaller contribution. In any case, it is necessary to give a realistic estimation of its value as it can give us additional information on the baryn-baryon interaction as compared to the other channels.
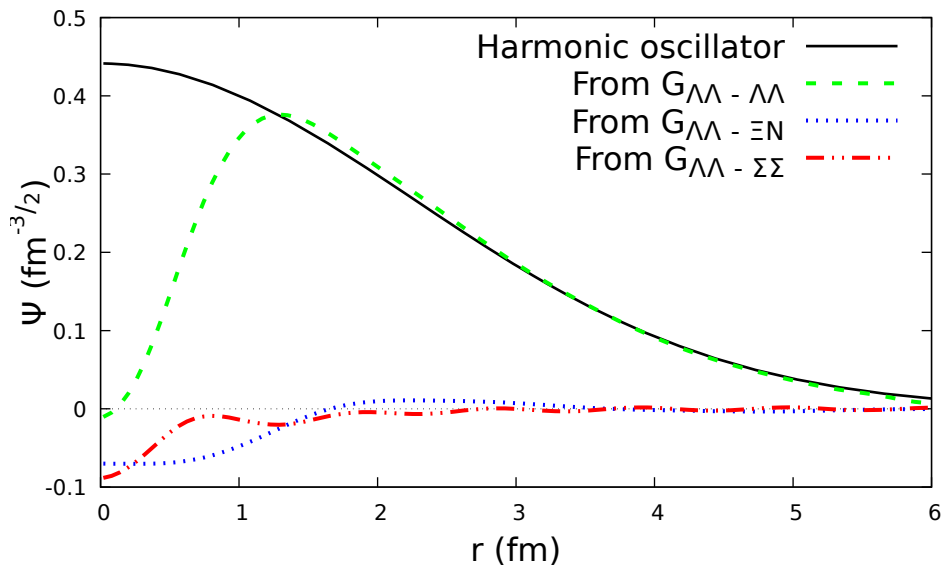

Figure 1: Comparison of the harmonic oscillator $\Lambda\Lambda$ radial wave function in $^{6}_{\Lambda\Lambda}$He with the different components of this same wave function obtained from a G-matrix calculation, and corresponding to the $^{1}S_{0}$ channel for a value of the relative momentum of 100 MeV. Figure taken from Ref.[9]

In the present work we study the $(\Lambda\Lambda - \Sigma\Sigma) \rightarrow YN$ decay mode in $^{6}_{\Lambda\Lambda}$He . To describe the weak transition we use a one-meson-exchange model which includes the contribution of the pseudoscalar π and η mesons. The evaluation of the corresponding Feynman amplitude requires the knowledge

of a set of strong and weak baryon-baryon-meson coupling constants. Only the ones involving decays into pions with enough phase-space can be directly extracted from experiments. To obtain the rest of couplings one must use effective lagrangians, based on the use of SU(3) flavor symmetry, formulated for the strong and weak interaction among hadrons.

For an easier understanding of the diagrams we are using, the baryons and mesons relevant for this work are shown in Tables I and II [11]. Due to the lack of time, K mesons are not considered in the present work and their inclusion is postponed.

The structure of this master thesis is the following. In Chapter II the expression for the decay rate is presented. In Chapter III the One Meson Exchange model used in our calculations of the two-body weak transition is explained, including the representation of the exchange diagrams and corresponding strong and weak vertices. Once the weak transition potential is derived, the coupling constants are computed using effective lagrangians and the pole model. Last two sections of Chaper III are dedicated to obtain the matrix elements for the isospin and the spin operators. Finally, in Chapter IV we discuss the results obtained and present some conclusions. We have added some appendices at the end to illustrate some specific computations, as well as the integral for the radial contributions.

Particle	Q	Quark composition	I	I_3	S	Mass (MeV)	Mean Life τ (s)	Non-Leptonic Decay Modes
Λ	0	uds	0	0	-1	1115.683 ± 0.006	$(2.632 \pm 0.020) \cdot 10^{-10}$	$p\pi^-$ / $n\pi^0$
Σ^0	0	uds	1	0	-1	1192.642 ± 0.024	$(7.4 \pm 0.07) \cdot 10^{-20}$	-
Σ^+	1	uus	1	1	-1	1189.37 ± 0.07	$(0.8018 \pm 0.0026) \cdot 10^{-10}$	$p\pi^0$ / $n\pi^+$
Σ^-	-1	dds	1	-1	-1	1197.449 ± 0.030	$(1.479 \pm 0.011) \cdot 10^{-10}$	$n\pi^-$
n	0	udd	$\frac{1}{2}$	$-\frac{1}{2}$	0	939.565413 ± 0.000006	880.2 ± 1.0	-
p	1	uud	$\frac{1}{2}$	$\frac{1}{2}$	0	938.272081 ± 0.000006	$> 2 \cdot 10^{29}$ (years)	-

Table I: Physical properties of the $(J^P) = (\frac{1}{2}^+)$ baryons used in the present work.

Particle	Q	Quark composition	I	I_3	S	Mass (MeV)	Mean Life τ (s)
π^0	0	$(u\bar{u} - d\bar{d})/\sqrt{2}$	1	0	0	134.9770 ± 0.0005	$(8.52 \pm 0.18) \cdot 10^{-17}$
π^+	1	$u\bar{d}$	1	1	0	139.57061 ± 0.00024	$(2.6033 \pm 0.0005) \cdot 10^{-8}$
π^-	-1	$d\bar{u}$	1	-1	0	139.57061 ± 0.00024	$(2.6033 \pm 0.0005) \cdot 10^{-8}$
η	0	$c_1(u\bar{u} - d\bar{d}) + c_2(s\bar{s})$	0	0	0	547.862 ± 0.017	-

Table II: Physical properties of the pseudoscalar $(J^P) = (0^-)$ mesons used in the present work.

II. Decay rate

The aim of this work is to obtain the decay rate expression of $\Lambda\Lambda$-hypernuclei when the $\Lambda\Lambda - \Sigma\Sigma$ strong coupled wave function is considered. The nonmesonic weak decay mechanism is studied within the one boson exchange model.

If we suppose that the initial hypernucleus is at rest, we can express our decay rate as [12]:

$$\Gamma = \int \frac{d^3k_1}{(2\pi)^3} \int \frac{d^3k_2}{(2\pi)^3} \sum_{m_1 m_2} \sum_{nuc.res} \frac{1}{2J+1} \sum_{M_J} (2\pi)\delta(E)|\mathcal{M}|^2, \tag{1}$$

where $\mathcal{M}$ is the nuclear transition amplitude $\mathcal{M} = < N\,Y\,^4Z|\hat{O}|^6_{\Lambda\Lambda}\text{He} >$ with $\hat{O}$ the two-body operator responsible of the transition $\Lambda\Lambda \to YN$, k_1 and k_2 are the two final particles momenta, J is the quantum number for the initial hypernucleus, M_J its projection and the $\delta(E)$ stands for the energy conservation. The first sum is over the spin projections of the two final particles whereas the second is over the quantum numbers of ^{4}He. The two initial integrals $\int \frac{d^3k_1}{(2\pi)^3} \int \frac{d^3k_2}{(2\pi)^3}(2\pi)\delta(E)$ are to be done over the two final particles, it is, over all final momenta possibilities.

To compute the weak transition amplitude, we need to decouple the $\Lambda\Lambda$ pair from the initial hypernuclear wave function. This is relatively simple, since the two $\Lambda's$ are weakly coupled to the residual ^{4}He core.

It is known experimentally that the $\Lambda\Lambda$ system has a quantum number $L = 0$, which contributes to the total wave function with a symmetric factor. Because these two particles are identical fermions, its compulsory for their total wave function to be antisymmetric. Then, an antisymmetric factor for the spin is needed, and therefore they must be coupled to $S = 0$.

$$|\Psi(^6_{\Lambda\Lambda}\text{He}) >= |^6_{\Lambda\Lambda}He >^{J=S=L=T=0} = |\Lambda\Lambda >^{J=S=L=T=0} \otimes |^4He >^{J=S=L=T=0} \tag{2}$$

Our final wave function contains the two baryons coming out from the two-body weak process, and a residual 4-particle state which has to coincide with the initial ^{4}He core, acting as spectator in the weak reaction.

$$\begin{aligned} < \Psi_f| \; &= \; < N|\otimes < Y|\otimes <^4 Z| = \\ &= \sum_{SM_S} < \frac{1}{2}m_1\frac{1}{2}m_2|SM_S >< SM_S| \sum_{TM_T} < \frac{1}{2}t_1T_2t_2|TM_T >< TM_T| < \vec{k}_N, \vec{k}_Y| <^4 Z| = \\ &= \sum_{SM_S}\sum_{TM_T} < \frac{1}{2}m_1\frac{1}{2}m_2|SM_S >< \frac{1}{2}t_1T_2t_2|TM_T >< SM_S| < TM_T| < \vec{k}_N, \vec{k}_Y| <^4 Z|. \end{aligned} \tag{3}$$

$\Delta I = 1/2$ variations in the weak transition can be incoporated through the coupling of the $|1/2 - 1/2 >$ isospurion to one of the Λ's in the initial $\Lambda\Lambda$ pair, that fixes the isospin state of the

couple to be $|1/2 - 1/2>$. Once this is done, isospin conservation can be implemented through the transition:

$$\sum_{SM_S} <\frac{1}{2}m_1\frac{1}{2}m_2|SM_S><\frac{1}{2}t_N T_Y t_Y|\frac{1}{2}-\frac{1}{2}><SM_S|<\frac{1}{2}-\frac{1}{2}|<\vec{k}_N,\vec{k}_Y|<^4 \text{Z}|. \tag{4}$$

The amplitude $\mathcal{M}$ with both the initial and the final wave functions can be written, once we have performed the change to separate between the center of mass and the relative wavefunction:

$$\mathcal{M} = <\vec{k}_N S_N t_N, \vec{k}_Y S_Y t_Y; ^4\text{Z}|\hat{O}|^6_{\Lambda\Lambda}He>|\frac{1}{2}-\frac{1}{2}>=$$
$$= \sum_{SM_S} <\frac{1}{2}m_1\frac{1}{2}m_2|SM_S><\frac{1}{2}t_N T_Y t_Y|\frac{1}{2}-\frac{1}{2}><\vec{K}|\psi^{CM}>$$
$$\times <\vec{k},SM_S,\frac{1}{2}-\frac{1}{2}|\hat{O}|\psi^{REL},S_0=0\,M_{S0}=0,\frac{1}{2}-\frac{1}{2}><^4\text{Z}|^4He>. \tag{5}$$

Introducing this on the expression for the decay rate we can do more simplifications:

$$\Gamma = \int \frac{d^3k}{(2\pi)^3}\int \frac{d^3K}{(2\pi)^3}\sum_{m_1 m_2}\sum_{nuc.res}\frac{1}{2J+1}\sum_{m_J}(2\pi)\delta(E)|M|^2 =$$
$$= \int \frac{d^3k}{(2\pi)^3}\int \frac{d^3K}{(2\pi)^3}\sum_{m_1 m_2}\sum_{nuc.res}\frac{1}{2J+1}\sum_{m_J}(2\pi)\delta(E)$$
$$\times |\sum_{SM_S} <\frac{1}{2}m_1\frac{1}{2}m_2|SM_S><\frac{1}{2}t_1 T_2 t_2|\frac{1}{2}-\frac{1}{2}><\vec{K}|\psi^{CM}>$$
$$\times <\vec{k},SM_S,\frac{1}{2}-\frac{1}{2}|\hat{O}(S)|\psi^{REL},S_0=0\,M_{S0}=0,\frac{1}{2}-\frac{1}{2}><^4\text{Z}|^4He>|^2. \tag{6}$$

Where we can take out the $2J+1=1$ term. As we previously explained, the total angular momenta for the $\Lambda\Lambda$ system is $J=0$. Also with $J(^4\text{He})=0$, we only have the $J(^6_{\Lambda\Lambda}\text{He}=0$ possibility. Firstly, $<^4\text{Z}|^4He>$ becomes a δ_{ZHe} that forces $Z=\text{He}$. Secondly, we do a simplification on the sums over the spin. This can be done taking out the Clebsch-Gordan coefficients for the spin outside the square value of $\mathcal{M}$ to obtain a single and easier expression:

$$\sum_{m_1 m_2}\sum_{SM_S} <\frac{1}{2}m_1\frac{1}{2}m_2|SM_S>\sum_{S'M'_S}<\frac{1}{2}m_1\frac{1}{2}m_2|S'M'_S>=\sum_{SM_S}\delta_{SS'}\delta_{M_S M'_S}. \tag{7}$$

So now the decay rate becomes:

$$
\begin{aligned}
\Gamma &= \int \frac{d^3k}{(2\pi)^3} \int \frac{d^3K}{(2\pi)^3} (2\pi)\delta(E) \sum_{SM_S} |<\frac{1}{2}t_N T_Y t_Y|\frac{1}{2} -\frac{1}{2}> \\
&\times <\vec{K}|\psi^{CM}><\vec{k}, SM_S, \frac{1}{2} -\frac{1}{2}|\hat{O}|\psi^{REL}, S_0 = 0\, M_{S0} = 0, \frac{1}{2} -\frac{1}{2}>|^2 = \\
&= \int \frac{d^3k}{(2\pi)^3} \int \frac{d^3K}{(2\pi)^3} (2\pi)\delta(E)|<\frac{1}{2}t_N T_Y t_Y|\frac{1}{2} -\frac{1}{2}>|^2|<\vec{K}|\psi^{CM}>|^2 \\
&\times \sum_{SM_S} |<\vec{k}, SM_S|\hat{O}(S)|\psi^{REL}, S_0 = 0\, M_{S0} = 0>|^2|<\frac{1}{2} -\frac{1}{2}|\hat{O}(T)|\frac{1}{2} -\frac{1}{2}>|^2. \quad (8)
\end{aligned}
$$

Where we have factorized some terms to compute them individually.

The first block $<\frac{1}{2}t_N T_Y t_Y|\frac{1}{2} -\frac{1}{2}>$ is the Clebsch-Gordan value resulting when coupling the two final isospin values to the only possibility $T = \frac{1}{2}$, $t = -\frac{1}{2}$.

$<\vec{K}|\psi^{CM}>$ is the corresponding overlaping factor between final and initial CM wave function. Similarly, we have $<\vec{k}, SM_S|\hat{O}|\psi^{REL}, S_0 = 0\, M_{S0} = 0>$, the ovelaping factor between relative initial and final wave function, which contains spatial and spin combinations. This is going to give us some restriction to other quantum numbers once the spin operator is applied.

Finally, $<\frac{1}{2} -\frac{1}{2}|\hat{O}(T)|\frac{1}{2} -\frac{1}{2}>$ is the isospin term.

We develop all these terms in the next sections.

III.   One Meson Exchange Model

To compute the decay rate we use a One Meson Exchange Model, which has been successful in describing the decay of single-Λ hypernuclei as well as previous calculations of the decay of $\Lambda\Lambda$ hypernuclei.

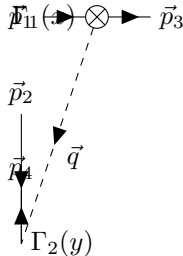Figure 2: General representation of the Feynman diagram for the weak $\Sigma\Sigma \to YN$ transition.

To derive the corresponding potential we start from the free Feynman amplitude depicted in the diagram shown in Figure 2, which can be expressed as:

$$\mathcal{M} = \int d^4x d^4y \bar{\psi}_3(x)\Gamma_1\psi_1(x)\Delta_M(x-y)\bar{\psi}_4(y)\Gamma_2\psi_2(y)\,, \tag{9}$$

where $\psi_p(x) = e^{-ipx}u(p)$ are the free baryon fields, Γ_i the operators describing the baryon-baryon-meson dynamics involved in each of the vertices, and Δ_M the meson propagator:

$$\Delta_m(x-y) = \int \frac{d^4q}{(2\pi)^4}\frac{e^{iq(x-y)}}{(q^0)^2 - \vec{q}^2 - m_m^2}\,. \tag{10}$$

Performing a change to center-of-mass and relative variables and integrating over the center-of-mass, time and energy variables, one obtains an expression that, in the non relativistic limit, gives us the Fourier transform of the transition potential in coordinate space $V(\vec{r})$:

$$V(\vec{r}) = -\int d^3r e^{i(\vec{p}_1-\vec{p}_3)\cdot\vec{r}} \int \frac{d^3q}{(2\pi)^3}\bar{u}(p_3)\Gamma_1 u(p_1)\frac{e^{-i\vec{q}\vec{r}}}{\vec{q}^2 + m_m^2}\bar{u}(p_4)\Gamma_2 u(p_2). \tag{11}$$

With this expression, we are in a position to obtain the weak transition potential for each of the specific exchange mechanisms shown in Figs. 3 and 4.
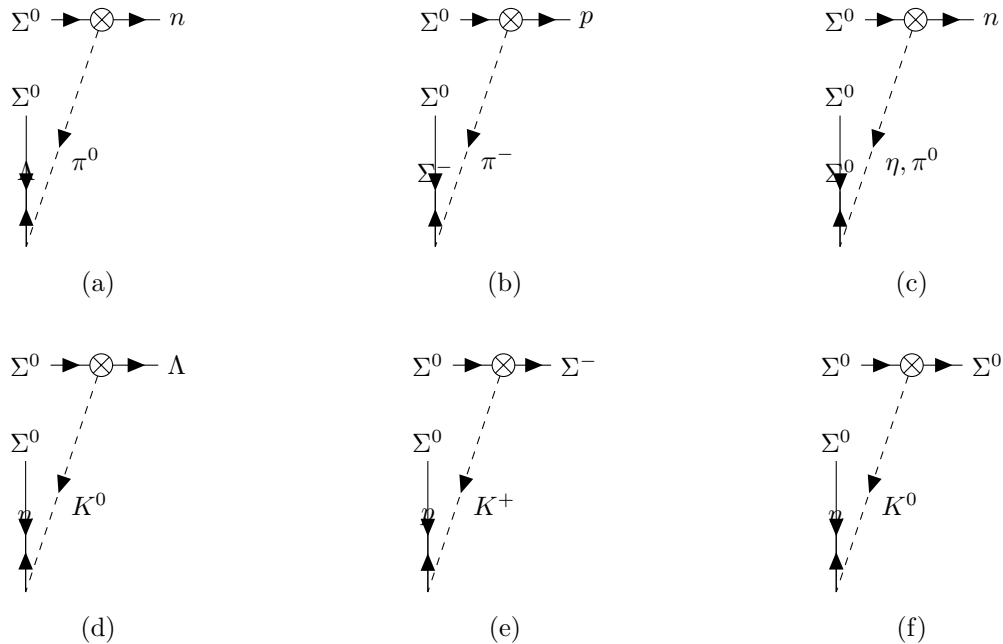
Figure 3: Feynman diagrams for the possible weak transitions starting from an initial $\Sigma^0\Sigma^0$ pair.

A. Exchange Diagrams

Since our work focusses on the effects of the $\Lambda\Lambda - \Sigma\Sigma$ component of the initial wave function to the decay rate, only weak transitions with an initial $\Sigma\Sigma$ state are considered. Figure 2 represents the transition from an initial $\Sigma_1\Sigma_2$ state (with the subindices denoting different charge) to a final NY state, with $Y = \Lambda$ or Σ. The crossed circle stands for the weak vertex while the strong vertex is generally denoted by a little full circle or without a symbol, as it is presented here. Both vertices must conserve charge. The strong vertex must preserve quark flavor and isospin, while the weak vertices follow the $\Delta I = 1/2$ rule and can change the quark flavor. The dashed line represents the exchange of a meson between the two vertices, i.e. the particle that will mediate the transition. The convention is to take Its direction towards the strong vertex. The structure of the Γ operators in Eq. (11) depends on the type of particles involved in each of the vertices.

Taking into account all these restrictions, we end up with the Feynman diagrams included in Figs. 3 and 4, representing weak decays starting from neutral Σ^0 or charged $\Sigma^{(+,-)}$ hyperons.

(a)　　　　　　　　　　(b)　　　　　　　　　　(c)

(d)　　　　　　　　　　(e)
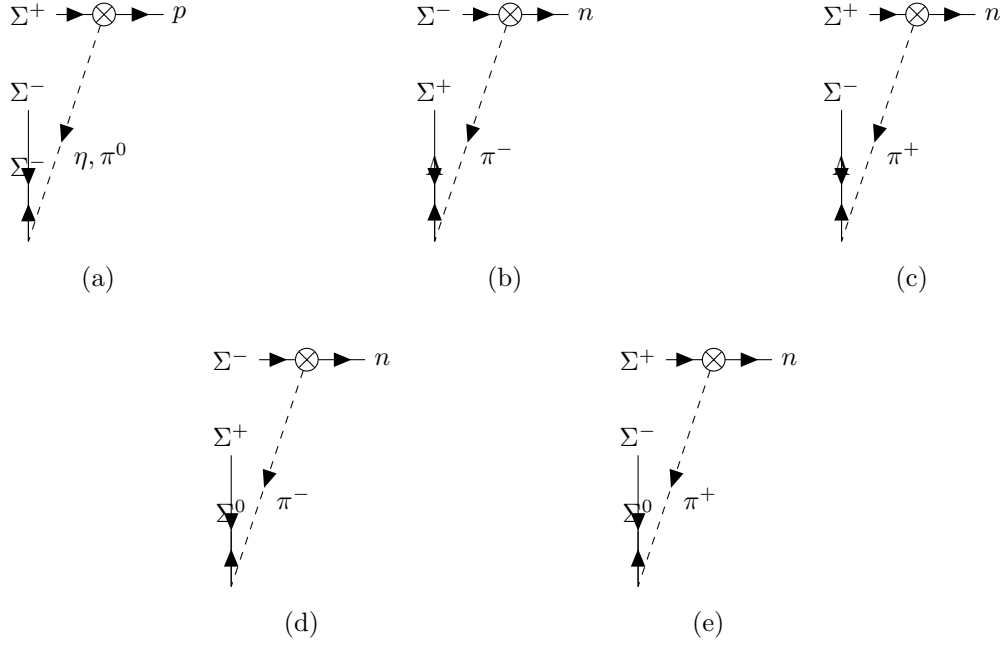
B.   Vertices and Final Potential Expression

For π and η meson exchanges we have a similar structure for weak and strong Hamiltonians except for isospin and coupling constants.

As it is said before, the nonrelativistic limit of the free space Feynman amplitude can be associated with the transition potential. So, what we need to calculate is the potential associated from the Hamiltonians we have at each vertex.

For this, we are going to need both strong and weak Hamiltonians, one of each associated at the corresponding vertex. For the strong Hamiltonian we use the usual $g_S\gamma_5$ parametrization, where g_S stands for the strong baryon-baryon-meson coupling, which will be given later on. For the weak vertex we need to incorporate two terms which will lead to the partity-violating (PV) piece ("A" term) and the parity conserving (PC) one ("B" term): $G_W^2(A + B\gamma_5)$.
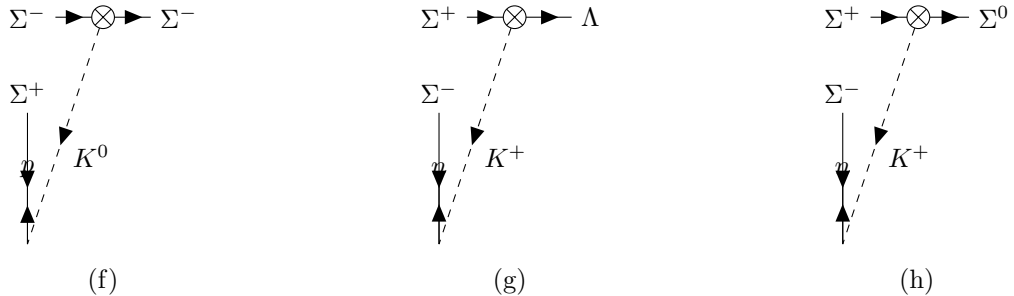

(f)　　　　　　　　　　(g)　　　　　　　　　　(h)

Figure 4: Feynman diagrams for the possible weak transitions starting from an initial $\Sigma^-\Sigma^+$ pair.

The propagator for the mesons is:

$$\frac{1}{q^2 - m_m^2} = \frac{1}{q_0^2 - \vec{q}^2 - m_m^2} \overset{n.r.}{=} \frac{-1}{\vec{q}^2 + m_m^2}, \tag{12}$$

where $\vec{q}$ is the momentum carried by the meson directed towards the strong vertex.

The terms needed are:

$$\begin{aligned}
\bar{\psi}_N(\vec{k}')A\psi_{\Sigma_1}(\vec{k}) &= \sqrt{\frac{E'+M}{2E'}}\left(1 \quad -\frac{\vec{\sigma_1}\cdot\vec{k}'}{E'+M}\right) A\sqrt{\frac{E+M_{\Sigma_1}}{2E}}\begin{pmatrix}1\\ \frac{\vec{\sigma_1}\cdot\vec{k}}{E+M_{\Sigma_1}}\end{pmatrix} = \\
&= A\sqrt{\frac{(E'+M)(E+M_{\Sigma_1})}{4EE'}}\left(1 - \frac{(\vec{\sigma_1}\cdot\vec{k}')(\vec{\sigma_1}\cdot\vec{k})}{(E'+M)(E+M_{\Sigma_1})}\right) \overset{M=M_{\Sigma_1}=\bar{M}}{=} \\
&= A\sqrt{\frac{(E'+\bar{M})(E+\bar{M})}{4EE'}}\left(1 - \frac{(\vec{\sigma_1}\cdot\vec{k}')(\vec{\sigma_1}\cdot\vec{k})}{(E'+\bar{M})(E+\bar{M})}\right) \overset{E=E'}{=} \\
&= A\sqrt{\frac{(E+\bar{M})^2}{4E^2}}\left(1 - \frac{(\vec{\sigma_1}\cdot\vec{k}')(\vec{\sigma_1}\cdot\vec{k})}{(E+\bar{M})^2}\right) \overset{E=\bar{M}}{=} \\
&= A\left(1 - \frac{(\vec{\sigma_1}\cdot\vec{k}')(\vec{\sigma_1}\cdot\vec{k})}{4\bar{M}^2}\right) \overset{L.O.}{=} A. \tag{13}
\end{aligned}$$

$$\begin{aligned}
\bar{\psi}_Y(-\vec{k}')\gamma_5\psi_{\Sigma_2}(-\vec{k}) &= \sqrt{\frac{E'+M_Y}{2E'}}\left(1 \quad \frac{\vec{\sigma_2}\cdot\vec{k}'}{E'+M_Y}\right)\begin{pmatrix}0 & \mathbb{I}\\ \mathbb{I} & 0\end{pmatrix}\sqrt{\frac{E+M_{\Sigma_2}}{2E}}\begin{pmatrix}1\\ \frac{-\vec{\sigma_2}\cdot\vec{k}}{E+M_{\Sigma_2}}\end{pmatrix} \overset{M_{\Sigma_2}=M_Y=M}{=} \\
&= \sqrt{\frac{(E'+M)(E+M)}{4EE'}}\left(\frac{\vec{\sigma_2}\cdot\vec{k}'}{E'+M} \quad 1\right)\begin{pmatrix}1\\ \frac{-\vec{\sigma_2}\cdot\vec{k}}{E+M}\end{pmatrix} = \\
&= \sqrt{\frac{(E'+M)(E+M)}{4EE'}}\left(\frac{\vec{\sigma_2}\cdot\vec{k}'}{E'+M} - \frac{\vec{\sigma_2}\cdot\vec{k}}{E+M}\right) \overset{(E=E')}{=} \\
&= \frac{\vec{\sigma_2}\cdot\vec{k}' - \vec{\sigma_2}\cdot\vec{k}}{2E} = \frac{1}{2E}\vec{\sigma_2}\cdot(\vec{k}'-\vec{k}) \overset{E=M}{=} -\frac{1}{2M}(\vec{\sigma_2}\cdot\vec{q}). \tag{14}
\end{aligned}$$

The PC term can be obtained as in the previous case, leading as final result:

$$\begin{aligned}
\bar{\psi}_N(\vec{k}')B\gamma_5\psi_{\Sigma_1}(\vec{k}) &= B\sqrt{\frac{(E'+M)(E+M_{\Sigma_1})}{4EE'}}\left(-\frac{\vec{\sigma_1}\cdot\vec{k}'}{E'+M} + \frac{\vec{\sigma_1}\cdot\vec{k}}{E+M_{\Sigma_1}}\right) \overset{M=M_{\Sigma_1}=\bar{M}}{=} \\
&= B\frac{(\bar{E}+\bar{M})}{2\bar{E}}\left(\frac{\vec{\sigma_1}\cdot\vec{q}}{\bar{E}+\bar{M}}\right) \overset{E=\bar{M}}{=} B\frac{\vec{\sigma_1}\cdot\vec{q}}{2\bar{M}}. \tag{15}
\end{aligned}$$

Combining Eqs. (13), (12) and (14), and taking the leading contribution, we obtain the PV potential:

$$V_{PV}(\vec{q}) \sim \frac{1}{\vec{q}^2 + m_m^2}A\frac{1}{2M}(\vec{\sigma_2}\cdot\vec{q}) \overset{\bar{E}\approx\bar{M}}{=} \frac{1}{\vec{q}^2 + m_m^2}\frac{A}{2M}(\vec{\sigma_2}\cdot\vec{q}). \tag{16}$$

Analogously, the combination of Eqs. (14), (12) and (15), leads us to the leading PC potential:

$$V_{PC}(\vec{q}) \sim B\frac{\vec{\sigma_1}\cdot\vec{q}}{2\bar{M}}\frac{1}{\vec{q}^2 + m_m^2}\frac{1}{2M}(\vec{\sigma_2}\cdot\vec{q}). \tag{17}$$

The potential is the sum of these two terms including $G_W^2 g_S$ factor and the isospin operator, which will be given at the end of this section:

$$
\begin{aligned}
V_m(\vec{q}) &= -G_W^2 g_S \left[\frac{1}{\vec{q}^2 + m_m^2} \frac{A}{2M} (\vec{\sigma}_2 \cdot \vec{q}) + B \frac{\vec{\sigma}_1 \cdot \vec{q}}{2\bar{M}} \frac{1}{\vec{q}^2 + m_m^2} \frac{1}{2E} (\vec{\sigma}_2 \cdot \vec{q}) \right] \hat{O}(T) = \\
&= -G_W^2 g_S \frac{1}{\vec{q}^2 + m_m^2} \frac{1}{2M} (\vec{\sigma}_2 \cdot \vec{q}) \left(A + B \frac{\vec{\sigma}_1 \cdot \vec{q}}{2\bar{M}} \right) \hat{O}(T) .
\end{aligned}
\tag{18}
$$

In order to calculate the transition amplitude we have to perform a Fourier transformation. The calculation of the PV contribution is given by:

$$
V'(\vec{r}) = \frac{1}{(2\pi)^3} \int \frac{e^{i\vec{q}\vec{r}}}{\vec{q}^2 + m^2} (\vec{\sigma} \cdot \vec{q}) d^3q = \frac{\sigma_j \nabla_j}{i(2\pi)^3} \int \frac{e^{i\vec{q}\vec{r}}}{\vec{q}^2 + m^2} d^3q = \frac{-1}{4i\pi} (\vec{\sigma}_2 \cdot \hat{r}) \frac{e^{-mr}}{r} (m + \frac{1}{r}) ,
\tag{19}
$$

which can be solved using the Cauchy's residue theorem.

The PC potential in r-space is similarly calculated:

$$
V''(\vec{r}) = \frac{1}{(2\pi)^3} \int \frac{e^{i\vec{q}\vec{r}}}{\vec{q}^2 + m^2} (\vec{\sigma}_1 \cdot \vec{q})(\vec{\sigma}_2 \cdot \vec{q}) d^3q.
\tag{20}
$$

Here we use the relation $(\vec{\sigma}_1 \cdot \vec{q})(\vec{\sigma}_2 \cdot \vec{q}) = \{\sigma_1 q \sigma_2 q - \frac{1}{3}\sigma_1\sigma_2 q^2\} + \frac{1}{3}\sigma_1\sigma_2 q^2 = S_{12} + \frac{1}{3}\sigma_1\sigma_2 q^2$ to split the PC potential in a central and a tensor contribution. Note that, as explained in section [III E], the tensor operator will not contribute because the $\Sigma\Sigma$ system is in the singlet state.

Again, using the Cauchy's residue theorem, we obtain the PC potential

$$
V''(\vec{r}) = \frac{\sigma_1\sigma_2}{3(2\pi)^3} \frac{2\pi}{ir} \int_{-\infty}^{\infty} \frac{e^{iqr}}{\vec{q}^2 + m^2} q^3 dq = -\frac{\sigma_1\sigma_2}{6\pi} \frac{e^{-mr}}{r} m^2.
\tag{21}
$$

The final potential then becomes

$$
\begin{aligned}
V(\vec{r}) &= -G_W^2 g_S \left[-\frac{A}{2M} \left(\frac{1}{4i\pi} (\vec{\sigma}_2 \cdot \hat{r}) \frac{e^{-mr}}{r} (m + \frac{1}{r}) \right) + \frac{B}{2\bar{M}2M} \left(-\frac{\sigma_1\sigma_2}{6\pi} \frac{e^{-mr}}{r} m^2 \right) \right] \hat{O}(T) = \\
&= -G_W^2 g_S \frac{1}{2M4\pi} \frac{e^{-mr}}{r} \left[-A \left(\frac{1}{i} (\vec{\sigma}_2 \cdot \hat{r})(m + \frac{1}{r}) \right) + \frac{B}{\bar{M}} \left(-\frac{\sigma_1\sigma_2}{3} m^2 \right) \right] \hat{O}(T) .
\end{aligned}
\tag{22}
$$

Both PC and PV contributions can be splited in three terms: one containing the spin operator, another for the isospin one, and a final term including all radial dependences. For our case:

$$
V(\vec{r}) = \left[\vec{\sigma}_1 \vec{\sigma}_2 \hat{V}_{SS}(r) + \vec{\sigma}_2 \cdot \hat{r} V_{PV}(r) \right] \hat{O}(T),
\tag{23}
$$

$$
V_{SS} = G_W^2 g_S \frac{B}{2\bar{M}2M} \frac{1}{3} \left(\frac{e^{-mr}}{2\pi r} m^2 \right)
$$

$$
V_{PV}(r) = G_W^2 g_S \frac{A}{2M} m \frac{e^{-mr}}{4i\pi r} \left(1 + \frac{m}{r} \right),
\tag{24}
$$

where $\hat{O}(T)$ is the isospin operator.

To obtain the isospin matrix elements we enforce the $\Delta T = \frac{1}{2}$ rule through the coupling of isospurion to the initial hyperon in the weak vertex

$$|\tilde{Y}> \equiv |\frac{1}{2} - \frac{1}{2}> \otimes |Y>. \tag{25}$$

Given that the Σ is an isospin triplet, the coupling with the isospurion gives us two spurion states, one with $T = 1/2$ and the other with $T = 3/2$:

$$|\tilde{\Sigma}^-> = |\Sigma^-> \otimes \begin{pmatrix} 0 \\ 1 \end{pmatrix} = |\frac{1}{2} - \frac{1}{2}> \otimes |1 - 1> = |\frac{3}{2} - \frac{3}{2}>$$

$$|\tilde{\Sigma}^0> = |\Sigma^0> \otimes \begin{pmatrix} 0 \\ 1 \end{pmatrix} = |\frac{1}{2} - \frac{1}{2}> \otimes |10> = \sqrt{\frac{2}{3}}|\frac{3}{2} - \frac{1}{2}> + \frac{1}{\sqrt{3}}|\frac{1}{2} - \frac{1}{2}>$$

$$|\tilde{\Sigma}^+> = |\Sigma^+> \otimes \begin{pmatrix} 0 \\ 1 \end{pmatrix} = |\frac{1}{2} - \frac{1}{2}> \otimes |11> = \frac{1}{\sqrt{3}}|\frac{3}{2}\frac{1}{2}> + \sqrt{\frac{1}{3}}|\frac{1}{2}\frac{1}{2}>. \tag{26}$$

Since we are only considering the exchange of non-strange mesons (π, η), the $\Sigma\Sigma \to YN$ transition will always have the weak vertex located in the ΣN baryonic line. This vertex can be expressed as

$$M_{\Sigma \to Nm} = \left[\bar{\psi}_N(A^{\Sigma\frac{1}{2}} + B^{\Sigma\frac{1}{2}}\gamma_5) + \bar{\psi}_N(A^{\Sigma\frac{3}{2}} + B^{\Sigma\frac{3}{2}}\gamma_5)\right]\hat{O}(T) \cdot \vec{\Phi}_m\tilde{\Sigma}, \tag{27}$$

where the first term represents the decay from the isospin $1/2$ of the Σ spurion, and the second one involves T instead of τ, that is the decay from the isospin $3/2$ component of the Σ spurion. Only when a π is the meson being interchanged this two cases will appear in contraposition with the η case, where the isospin can only come from a $1/2 \to 1/2$ transition. This is explained more accurately in section [III D].

Putting together all the contributions the final potential is given by

$$V_\Sigma(\vec{q}) = -G_F m_m^2 \frac{g_S}{2M} \left[\left(A^{\Sigma\frac{1}{2}} + \frac{B^{\Sigma\frac{1}{2}}}{2\bar{M}}\vec{\sigma}_1\vec{q}\right) + \left(A^{\Sigma\frac{3}{2}} + \frac{B^{\Sigma\frac{3}{2}}}{2\bar{M}}\vec{\sigma}_1\vec{q}\right)\right]\hat{O}(T)\frac{\vec{\sigma}_2\vec{q}}{\vec{q}^2 + m_m^2}. \tag{28}$$

Where $G_F m_m^2 = G_W^2$. Now we apply the same relation as before $((\vec{\sigma}_1 \cdot \vec{q})(\vec{\sigma}_2 \cdot \vec{q}) = \{\sigma_1 q \sigma_2 q - \frac{1}{3}\sigma_1\sigma_2 q^2\} + \frac{1}{3}\sigma_1\sigma_2 q^2 = S_{12} + \frac{1}{3}\sigma_1\sigma_2 q^2)$, and do a Fourier transform to obtain the potential decomposition as before.

The structure is the same, but taking into account that we have two different options for each

isospin operator.

$$V_{SS}^{1/2}(r) \;=\; G_F^2 \frac{B^{1/2}}{2\bar{M}2M} \frac{1}{3} \left(\frac{e^{-mr}}{2\pi r} m^2 \right)$$

$$V_{PV}^{1/2}(r) \;=\; G_F^2 g \frac{A^{1/2}}{2M} m \frac{e^{-mr}}{4i\pi r} \left(1 + \frac{m}{r} \right)$$

$$V_{SS}^{3/2}(r) \;=\; G_F^2 \frac{B^{3/2}}{2\bar{M}2M} \frac{1}{3} \left(\frac{e^{-mr}}{2\pi r} m^2 \right)$$

$$V_{PV}^{3/2}(r) \;=\; G_F^2 g \frac{A^{3/2}}{2M} m \frac{e^{-mr}}{4i\pi r} \left(1 + \frac{m}{r} \right). \tag{29}$$

C. Coupling Constants

At this point, we must derive the values of the weak and strong baryon-baryon-meson ($BB\phi$) constants that appear in the expression of our potential. To do that, we will use the appropriate effective Lagrangians in each sector.

For the strong vertices the Lagrangian at lowest order is given by the expression:

$$\mathcal{L}^{strong} = \text{Tr}[\bar{B}(i\gamma^\mu\nabla_\mu - M_B)B] + \frac{D}{2}\text{Tr}[\bar{B}\gamma^\mu\gamma_5\{u_\mu, B\}] + \frac{F}{2}\text{Tr}[\bar{B}\gamma^\mu\gamma_5[u_\mu, B]], \tag{30}$$

with B and $\bar{B}$ the baryon and anti-baryon matrices:

$$B = \begin{pmatrix} \frac{1}{\sqrt{2}}\Sigma^0 + \frac{1}{\sqrt{6}}\Lambda & \Sigma^+ & p \\ \Sigma^- & -\frac{1}{\sqrt{2}}\Sigma^0 + \frac{1}{\sqrt{6}}\Lambda & n \\ \Xi^- & \Xi^0 & -\frac{2}{\sqrt{6}}\Lambda \end{pmatrix} \tag{31}$$

$$\bar{B} = \begin{pmatrix} \frac{1}{\sqrt{2}}\bar{\Sigma}^0 + \frac{1}{\sqrt{6}}\bar{\Lambda} & \bar{\Sigma}^- & \bar{\Xi}^- \\ \bar{\Sigma}^+ & -\frac{1}{\sqrt{2}}\bar{\Sigma}^0 + \frac{1}{\sqrt{6}}\bar{\Lambda} & \bar{\Xi}^0 \\ \bar{p} & \bar{n} & -\frac{2}{\sqrt{6}}\bar{\Lambda} \end{pmatrix}. \tag{32}$$

The operators appearing in Eq. (30) are defined as:

$$\nabla_\mu = \partial_\mu + [\Gamma_\mu, B]$$

$$u_\mu = i(u^\dagger\partial_\mu u - u\partial_\mu u^\dagger)$$

$$\Gamma_\mu = i(u^\dagger\partial_\mu u + u\partial_\mu u^\dagger). \tag{33}$$

The u matrix contains the meson fields, ϕ, through the expression :

$$u = e^{i\phi/\sqrt{2}f} \approx 1 + \frac{i}{\sqrt{2}f}\phi(x)$$
$$u^\dagger = e^{-i\phi/\sqrt{2}f} \approx 1 - \frac{i}{\sqrt{2}f}\phi(x)^\dagger. \tag{34}$$

which has been expanded to first order to account for the exchange of a single meson. The explicit expressions for the meson matrix is:

$$\phi = \begin{pmatrix} \frac{1}{\sqrt{2}}\pi^0 + \frac{1}{\sqrt{6}}\eta & \pi^+ & K^+ \\ \pi^- & -\frac{1}{\sqrt{2}}\pi^0 + \frac{1}{\sqrt{6}}\eta & K^0 \\ K^- & \bar{K}^0 & -\frac{2}{\sqrt{6}}\eta \end{pmatrix}. \tag{35}$$

One can see that at lowest order, the contribution of the Γ_μ and u_μ terms are:

$$\Gamma_\mu = i(u^\dagger \partial_\mu u + u \partial_\mu u^\dagger) = 0 \tag{36}$$

and

$$u_\mu = i(u^\dagger \partial_\mu u - u \partial_\mu u^\dagger) = \frac{-\sqrt{2}}{f}\partial_\mu \phi, \tag{37}$$

allowing us to rewirte the first term in the Lagrangian of Eq.(30) as:

$$\bar{B}(i\gamma^\mu \nabla_\mu - M_B)B = i\bar{B}\gamma^\mu \nabla_\mu B - \bar{B}M_B B =$$
$$= i\bar{B}\gamma^\mu \partial_\mu B + i\bar{B}\gamma^\mu[\Gamma_\mu, b]B - \bar{B}M_B B = i\bar{B}\gamma^\mu \partial_\mu B - \bar{B}M_B B, \tag{38}$$

contributing only to the kinetic energy and the mass term of the baryons in diagonal channels. The $BB\phi$ coupling constants will be given by the second and third terms in Eq.(30), where the constants D and F are the octet baryon to meson couplings, with values $D = 0.85$ MeV, $F = 0.52$ MeV [13][14]. To exemplify the procedure we have added in Appendix (C 1) the explicit calculation of the strong $\Sigma^- \pi^+ \to \Sigma^0$ vertex. Our results for the strong coupling constants required to perform the present calculation, which includes only the exchange of the π and η mesons, are presented in Table III. Note that, for completeness, we have added the ones corresponding to the kaon, although its contribution has not been evaluated in the present work.

For the weak vertices, one must perform an equivalent calculation but using the appropriate weak lagrangian. It is important to note that the effective lagrangian can only give us the parity-violating coupling constants [15] because it does not contain the CP transformation properties needed to compute PC constants.

$$\mathcal{L}^{PV} = G_F m_\pi^2 \sqrt{2} f_\pi \left(h_D \mathrm{Tr}[\bar{B}\{\xi^\dagger h\xi, B\}] + h_F \mathrm{Tr}[\bar{B}[\xi^\dagger h\xi, B]] \right), \tag{39}$$

where $G_F m_\pi^2 = 2.21 \times 10^{-7}$, $f_\pi = 93$ (MeV) is the pion decay constant, $h_D = -1.69 \times 10^{-7}$ and $h_F = 3.26 \times 10^{-7}$ constants taken from [16], h is a matrix which effectively accounts for the change in strangeness,

$$h = \begin{pmatrix} 0 & 0 & 0 \\ 0 & 0 & 1 \\ 0 & 0 & 0 \end{pmatrix}, \tag{40}$$

and the meson fields are included in the ξ matrix in analogy with the u matrix appearing in the strong Lagrangian, giving at leading order:

$$\xi^\dagger h\xi = h + [h, \phi]\frac{i}{\sqrt{2}f}. \tag{41}$$

As before, an explicit example of the calculation is included in Appendix C 2, and the values of the relevant coupling constants for the weak sector are presented in Table V.

Channel	$\frac{D}{2}\text{Tr}[\bar{B}\gamma^\mu\gamma_5\{u_\mu, B\}] + \frac{F}{2}\text{Tr}[\bar{B}\gamma^\mu\gamma_5[u_\mu, B]]$	Numerical values
$\Sigma^-\pi^+ \to \Sigma^0$	$+\text{F}\gamma^\mu\gamma_5\bar{\Sigma}^0\partial_\mu\pi^+\Sigma^-\frac{1}{f}$	13.36
$\Sigma^+\pi^- \to \Sigma^0$	$-\text{F}\gamma^\mu\gamma_5\bar{\Sigma}^0\partial_\mu\pi^-\Sigma^+\frac{1}{f}$	- 13.32
$\Sigma^0\pi^0 \to \Sigma^0$	0	0
$\Sigma^0\eta \to \Sigma^0$	$\text{D}\gamma^\mu\gamma_5\bar{\Sigma}^0\partial_\mu\eta\Sigma^0\frac{1}{\sqrt{3}f}$	12.59
$\Sigma^0\pi^- \to \Sigma^-$	$\text{F}\gamma^\mu\gamma_5\bar{\Sigma}^-\partial_\mu\pi^-\Sigma^0\frac{1}{f}$	13.36
$\Sigma^0\pi^0 \to \Lambda$	$\text{D}\gamma^\mu\gamma_5\bar{\Lambda}\partial_\mu\pi^0\Sigma^0\frac{1}{\sqrt{3}f}$	12.18
$\Sigma^-\pi^+ \to \Lambda$	$+\text{D}\gamma^\mu\gamma_5\bar{\Lambda}\partial_\mu\pi^+\Sigma^-\frac{1}{\sqrt{3}f}$	12.21
$\Sigma^-\pi^0 \to \Sigma^-$	$-\text{F}\gamma^\mu\gamma_5\bar{\Sigma}^-\partial_\mu\pi^0\Sigma^-\frac{1}{f}$	-13.39
$\Sigma^+\pi^- \to \Lambda$	$\text{D}\gamma^\mu\gamma_5\bar{\Lambda}\partial_\mu\pi^-\Sigma^-\frac{1}{\sqrt{3}}f$	12.16
$\Sigma^0 K^0 \to n$	$-\text{D}\bar{n}\gamma^\mu\gamma_5\partial_\mu K^0\Sigma^0\frac{1}{2f} + \text{F}\bar{n}\gamma^\mu\gamma_5\partial_\mu K^0\Sigma^0\frac{1}{2f}$	-3.78
$\Sigma^0 K^+ \to p$	$\text{D}\bar{p}\gamma^\mu\gamma_5\partial_\mu K^+\Sigma^0\frac{1}{2f}$ $-\text{F}\bar{p}\gamma^\mu\gamma_5\partial_\mu K^+ K^0\frac{1}{2f}$	3.78
$\Sigma^+ K^0 \to p$	$\text{D}\bar{p}\gamma^\mu\gamma_5\partial_\mu K^0\Sigma^+\frac{1}{\sqrt{2}f}$ $-\text{F}\bar{p}\gamma^\mu\gamma_5\partial_\mu K^0 K^+\frac{1}{\sqrt{2}f}$	5.34
$\Sigma^- K^+ \to n$	$\text{D}\bar{n}\gamma^\mu\gamma_5\partial_\mu K^+\Sigma^-\frac{1}{\sqrt{2}f}$ $-\text{F}\bar{n}\gamma^\mu\gamma_5\partial_\mu K^+\Sigma^-\frac{1}{\sqrt{2}f}$	5.36
$\Sigma^-\eta \to \Sigma^-$	$\text{D}\bar{\Sigma}^-\gamma^\mu\gamma_5\partial_\mu\eta\Sigma^-\frac{1}{\sqrt{3}f}$	12.64

Table III: Values of the strong baryon-baryon-meson coupling constants involving pseudoscalar mesons. The numerical values are presented in terms of the corresponding baryons and meson.

The weak PC coupling constants can be obtained with the use of the pole model, as explained in Ref. [15]. To illustrate the method, we give the expression for the coupling entering the diagram depicted in Fig.(5), where the weak transition has been moved from the vertex to the corresponding baryon line. The first diagram on the right hand side of the figure represents the same weak process but with the weak transition shifted after the strong interaction takes place, while in the second diagram it is shifted onto the baryonic line right before the strong coupling occurs. The final expression for this particular vertex is given by:

$$g_{\Sigma^+\Lambda\pi^-}\frac{1}{m_n - m_\Lambda}A_{\Lambda n} + g_{\Sigma^+\Sigma^0\pi^-}\frac{1}{m_n - m_\Sigma^0}A_{\Sigma^0 n} + g_{pn\pi^-}\frac{1}{m_{\Sigma^+} - m_p}A_{\Sigma p}. \tag{42}$$

In the equation above, the g constants stand for the strong BBM couplings at each of the strong vertices, the denominator contains the mass difference between the baryons appearing in the baryon line where the weak vertex occurs, and the A take into account these weak transitions.

For this specific case, since the pion can connect two Σ baryons or a Σ and a Λ baryon through

Channel	$\frac{D}{2}\mathrm{Tr}[\bar{B}\gamma^{\mu}\gamma_5\{u_{\mu},B\}] + \frac{F}{2}\mathrm{Tr}[\bar{B}\gamma^{\mu}\gamma_5[u_{\mu},B]]$	Numerical value
$n\pi^0 \to n$	$\partial_{\mu}\pi^0(D+F)\frac{1}{2f}n\bar{n}$	13.84
$n\pi^+ \to p$	$\partial_{\mu}\pi^+(D+F)n\bar{p}\frac{1}{\sqrt{2}f}$	19.56
$\Sigma^0\pi^+ \to \Sigma^+$	$-\partial_{\mu}\pi^+\Sigma^0 F\bar{\Sigma}^+\frac{1}{f}$	-13.32
$\Sigma^0 K^- \to \Xi^-$	$\partial_{\mu}K - \Sigma^0(D+F)\bar{\Xi}^-\frac{1}{2f}$	18.52
$nK^- \to \Sigma^-$	$\partial_{\mu}K^-(D-F)n\bar{\Sigma}^-\frac{1}{\sqrt{2}f}$	5.36
$\Sigma^0\bar{K}^0 \to \Xi^0$	$\Sigma^0\partial_{\mu}\bar{K}^0\bar{\Xi}^0(D+F)\frac{1}{2f}$	18.47
$n\bar{K}^0 \to \Sigma^0$	$n\partial_{\mu}\bar{K}^0\bar{\Sigma}^0(-D+F)\frac{1}{2f}$	-3.78
$\Sigma^+\pi^0 \to \Sigma^+$	$F\Sigma^+\partial_{\mu}\pi^0\bar{\Sigma}^+\frac{1}{f}$	13.30
$p\pi^0 \to p$	$p\bar{p}\partial_{\mu}\pi^0(D+F)\frac{1}{2f}$	13.82
$p\pi^- \to n$	$p\partial_{\mu}\pi^-\bar{n}(D+F)\frac{1}{\sqrt{2}f}$	19.56
$\Sigma^-\bar{K}^0 \to \Xi^-$	$\Sigma^-\partial_{\mu}\bar{K}^0\bar{\Xi}^-(D+F)\frac{1}{\sqrt{2}f}$	26.24
$\Sigma^+ K^- \to \Xi^0$	$\Sigma^+\partial_{\mu}K^-\bar{\Xi}^-(D+F)\frac{1}{\sqrt{2}f}$	26.09
$pK^- \to \Lambda$	$-p\partial_{\mu}K^-\bar{\Lambda}(D+3F)\frac{\sqrt{3}}{6f}$	-15.37
$pK^- \to \Sigma^0$	$p\bar{\Sigma}^0\partial_{\mu}K^-(D-F)\frac{1}{2f}$	5.35
$n\eta \to n$	$-n\partial_{\mu}\eta\bar{n}(D-3F)\frac{\sqrt{3}}{6f}$	4.14

Table IV: Strong coupling constants entering the expression of the PC weak vertices through the pole model. The numerical values are presented in terms of the corresponding baryons and meson.

the strong interaction, we get an additional term, depicted as the third.

Channel	$h_D \text{Tr}[\bar{B}\{\xi^\dagger h\xi, B\}] + h_F \text{Tr}[\bar{B}[\xi^\dagger h\xi, B]]$	Numerical values
$\Sigma^0 \pi^0 \to n$	$-\frac{h_D - h_F}{2f}\Sigma^0(2f + i\pi^0)\bar{n}f_m G_F m_m^2$	4.95×10^{-7}
$\Sigma^0 \pi^+ \to p$	$-\frac{h_D - h_F}{\sqrt{2}f}\Sigma^0 i\pi^+ \bar{p}f_m G_F m_m^2$	3.50×10^{-7}
$\Sigma^0 \eta \to n$	$\frac{(h_D - h_F)}{2f}\Sigma^0(-2f + \sqrt{3}i\eta)\bar{n}f_m G_F m_m^2$	-4.29×10^{-7}
$\Sigma^0 \bar{K}^0 \to \Lambda$	$-\frac{h_D}{\sqrt{3}f}\Sigma^0 \bar{K}^0 i\bar{\Lambda}f_m G_F m_m^2$	9.75×10^{-8}
$\Sigma^0 K^- \to \Sigma^-$	$\frac{\sqrt{2}}{f}\Sigma^0 iK^- \bar{\Sigma^-}f_m G_F m_m^2$	4.61×10^{-7}
$\Sigma^0 \bar{K}^0 \to \Sigma^0$	$\frac{h_D}{f}\Sigma^0 \bar{K}^0 \bar{\Sigma}^0 if_m G_F m_m^2$	-1.69×10^{-7}
$\Sigma^+ \eta \to p$	$\frac{h_D - h_F}{\sqrt{2}f}(2f - \sqrt{i}\eta)\bar{p}\Sigma^+ f_m G_F m_m^2$	6.06×10^{-7}
$\Sigma^+ \pi^0 \to p$	$\frac{h_D - h_F}{\sqrt{2}f}(2f + i\pi^0)\bar{p}\Sigma^+ f_m G_F m_m^2$	-3.5×10^{-7}
$\Sigma^- \pi^+ \to n$	$-\frac{h_D - h_F}{f}i\bar{n}\Sigma^- \pi^+ f_m G_F m_m^2$	4.95×10^{-7}
$\Sigma^+ \pi^- \to n$	0	0
$\Sigma^- \bar{K}^0 \to \Sigma^-$	$\frac{h_D + h_F}{f}\bar{K}^0 i\bar{\Sigma^-}\Sigma^- f_m G_F m_m^2$	1.57×10^{-7}
$\Sigma^0 K^- \to \Lambda$	$\sqrt{\frac{2}{3}}h_D i\bar{\Lambda}K^- \Sigma^+ f_m G_F m_m^2$	-1.38×10^{-7}
$\Sigma^+ K^- \to \Sigma^0$	$-\frac{\sqrt{2}}{f}i\bar{\Sigma}^0 K^- \Sigma^+ f_m G_F m_m^2$	-4.61×10^{-7}

Table V: Values of the weak PV baryon-baryon-meson coupling constants involving pseudoscalar mesons. Note that, for completeness, we have added the ones corresponding to the kaon, although its contribution has not been evaluated in the present work. The numerical value is always the term containing the meson. The results are given in terms of $G_F m_m^2$ and the corresponding baryons and meson.

D. Isospin dependence

In analogy with the formalism presented in Ref. [9], we write the general structure of the isospin operator which enters Eq. (8) as:

$$
\begin{aligned}
&g_1 < \frac{1}{2}t_{Nf}, Tt_Y|\hat{O}_1|\frac{1}{2}t, T_2 t_2 >< \frac{1}{2}t|1t_1, \frac{1}{2} - \frac{1}{2} > + \\
&+g_2 < \frac{1}{2}t_{Nf}, Tt_Y|\hat{O}_2|\frac{3}{2}t, T_2 t_2 >< \frac{3}{2}t|1t_1, \frac{1}{2} - \frac{1}{2} > + \\
&+g_3 < \frac{1}{2}t_{Nf}, Tt_Y|\hat{O}_3|\frac{1}{2}t, T_2 t_2 >< \frac{1}{2}t|1t_1, \frac{1}{2} - \frac{1}{2} > ,
\end{aligned} \tag{43}
$$

where the Clebsh-Gordan coefficients on the right in each line represent the coupling of he isospurion ($|\frac{1}{2} - \frac{1}{2}\rangle$) to the Σ entering the weak vertex ($|1t_1\rangle$), to give an isospurion state ($\tilde{\Sigma}$) with isospin projection $t = t_1 - \frac{1}{2}$. We also recall here that $|T_2 t_2\rangle$ stands for the isospin state corresponding to
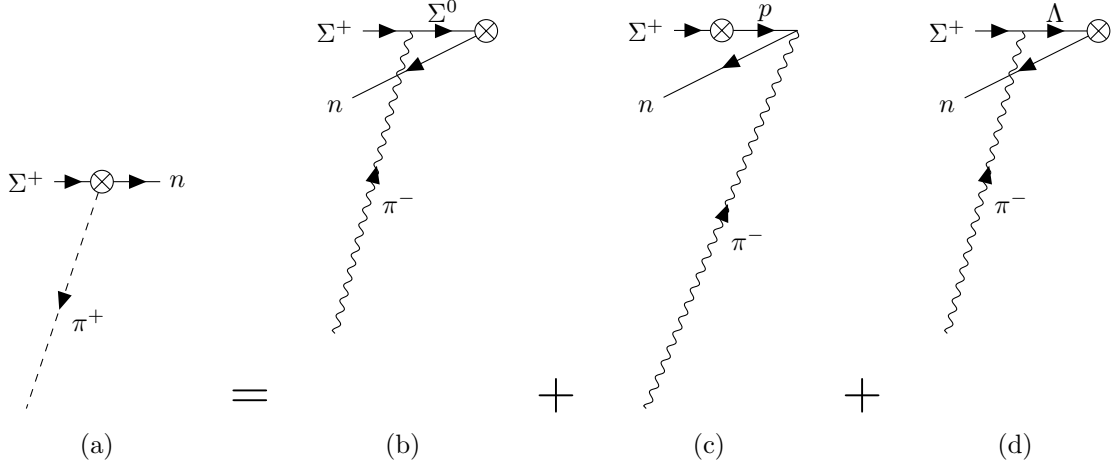
Figure 5: Ilustrative example of using a pole model.

Channel	$h_D \mathrm{Tr}[\bar{B}\{\xi^\dagger h\xi, B\}] + h_F \mathrm{Tr}[\bar{B}[\xi^\dagger h\xi, B]]$	Numerical value
$\Sigma^0 \pi^0 \to n$	$g_{nn\pi^0} \frac{1}{m_{\Sigma^0}-m_n} A_{\Sigma^0 n} + g_{\Sigma^0 \Sigma^0 \pi^0} \frac{1}{m_n - m_{\Sigma^0}} A_{\Sigma^0 n}$	2.25×10^{-5}
$\Sigma^0 \pi^+ \to p$	$g_{np\pi^+} \frac{1}{m_{\Sigma^0}-m_n} A_{\Sigma^0 n} + g_{\Sigma^0 \Sigma^+ \pi^+} \frac{1}{m_p - m_{\Sigma^+}} A_{\Sigma^+ p}$	9.80×10^{-8}
$\Sigma^0 \eta \to n$	$g_{nn\eta} \frac{1}{m_{\Sigma^0}-m_n} A_{\Sigma^0 n} + g_{\Sigma^0 \Sigma^0 \eta} \frac{1}{m_n - m_{\Sigma^0}} A_{\Sigma^0 n}$	-1.44×10^{-6}
$\Sigma^0 \bar{K}^0 \to \Lambda$	$g_{\Sigma^0 \Xi^0 \bar{K}^0} \frac{1}{m_\Lambda - m_{\Xi^0}} A_{\Xi^0 \Lambda} + g_{n\Lambda\Sigma^0 -m_n} \frac{1}{m_{\Sigma^0}-m_n} A_{\Sigma^0 n}$	1.21×10^{-6}
$\Sigma^0 K^- \to \Sigma^-$	$g_{\Sigma^0 \Xi^- K^-} \frac{1}{m_{\Sigma^-}-m_{\Xi^-}} A_{\Xi^- \Sigma^-} + g_{n\Sigma^- K^-} \frac{1}{m_{\Sigma^0}-m_n} A_{\Sigma^0 n}$	4.18×10^{-6}
$\Sigma^0 \bar{K}^0 \to \Sigma^0$	$g_{\Sigma^0 \Xi^0 \bar{K}^0} \frac{1}{m_{\Sigma^0}-m_{\Xi^0}} A_{\Xi^0 \Sigma^0} + g_{n\Sigma^0 \bar{K}^0} \frac{1}{m_{\Sigma^0}-m_n} A_{\Sigma^0 n}$	1.7×10^{-6}
$\Sigma^+ \eta \to p$	$g_{\Sigma^+ \Sigma^+ \eta} \frac{1}{m_p - m_{\Sigma^+}} A_{\Sigma^+ p} + g_{pp\eta} \frac{1}{m_{\Sigma^+}-m_p} A_{\Sigma^+ p}$	2.57×10^{-6}
$\Sigma^+ \pi^0 \to p$	$g_{\Sigma^+ \Sigma^+ \pi^0} \frac{1}{m_p - m_{\Sigma^+}} A_{\Sigma^+ p} + g_{pp\pi^0} \frac{1}{m_\Sigma^+ - m_p} A_{\Sigma^+ p}$	-1.26×10^{-7}
$\Sigma^- \pi^+ \to n$	$g_{\Sigma^- \Lambda \pi^+} \frac{1}{m_n - m_\Lambda} A_{\Lambda n} + g_{\Sigma^- \Sigma^0 \pi^+} \frac{1}{m_n - m_{\Sigma^0}} A_{\Sigma^0 n}$	-7.90×10^{-7}
$\Sigma^+ \pi^- \to n$	$g_{pn\pi^-} \frac{1}{m_{\Sigma^+}-m_p} A_{\Sigma^+ p} g_{\Sigma^+ \Lambda \pi^-} \frac{1}{m_n - m_\Lambda} A_{\Lambda n} + g_{\Sigma^+ \Sigma^0 \pi^-} \frac{1}{m_n - m\Sigma^0} A_{\Sigma^0 n}$	-9.99×10^{-7}
$\Sigma^- \bar{K}^0 \to \Sigma^-$	$g_{\Sigma^- \Xi^- \bar{K}^0} \frac{1}{m_{\Sigma^-}-m_{\Xi^-}} A_{\Xi^- \Sigma^-}$	6.70×10^{-6}
$\Sigma^0 K^- \to \Lambda$	$g_{\Sigma^+ \Xi^0 K^-} \frac{1}{m_\Lambda - m_{\Xi^0}} A_{\Xi^0 \Lambda} + g_{p\Lambda K^-} \frac{1}{m_{\Sigma^+}-m_p} A_{\Sigma^+ p}$	1.14×10^{-5}
$\Sigma^+ K^- \to \Sigma^0$	$g_{\Sigma^+ \Xi^0 K^-} \frac{1}{m_{\Sigma^0}-m_{\Xi^0}} A_{\Xi^0 \Sigma^0} + g_{p\Sigma^0 K^-} \frac{1}{m_{\Sigma^+}-m_p} A_{\Sigma^+ p}$	2.40×10^{-6}

Table VI: Values of the weak PC baryon-baryon-meson coupling constants involving pseudoscalar mesons. Note that, for completeness, we have added the ones corresponding to the kaon, although its contribution has not been evaluated in the present work.

the Σ entering the strong vertex, while $\langle \frac{1}{2} t_{Nf}|$ and $\langle Tt_Y|$ represent the final nucleon and hyperon

isospin states respectively.

The operational structures in Eq. (43) are:

$$\hat{O}_1 = \vec{\tau}_1 \cdot \vec{T}_2, \qquad \hat{O}_2 = \vec{T}_1 \cdot \vec{T}_2, \qquad \hat{O}_3 = \hat{I}_1 \cdot \hat{I}_2. \qquad (44)$$

but not all of them contribute to all final states. When our final state is given by a $n\Lambda$ pair we will only have contributions from the two first operators, due to the fact that the Λ has $T = 0$ and thus, it is not possible to connect the corresponding states with an identity operator. This is illustrated in Figure 6, where only the two possibilities that are allowed are drawn. All three operators contribute when the final state is $N\Sigma$, as shown in Figure 7.
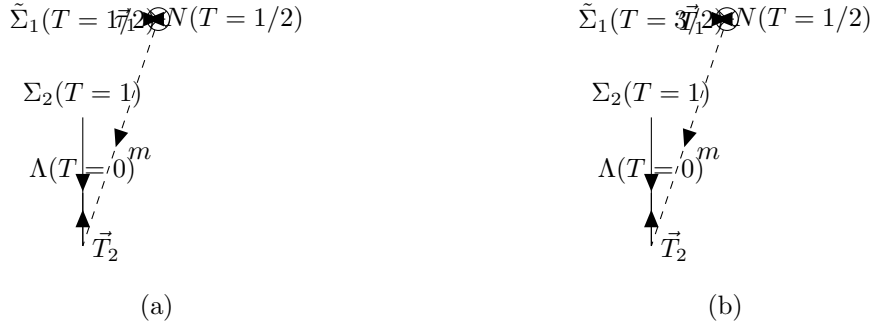
Figure 6: Diagrams showing the different operators that contribute to a final $n\Lambda$ state.
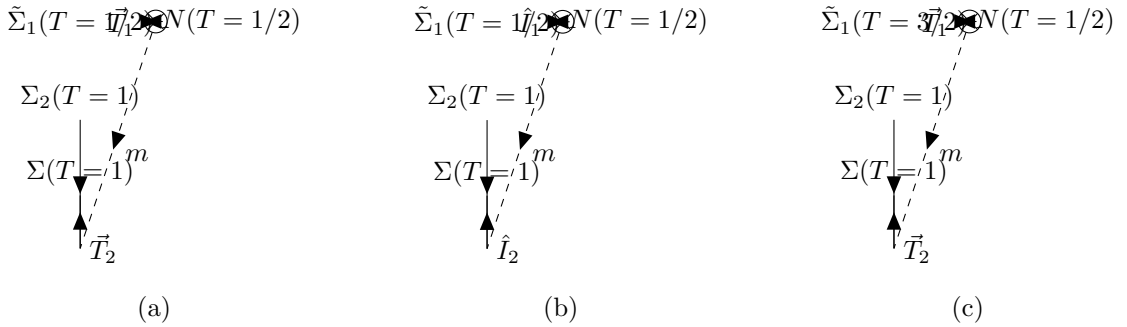

Figure 7: Diagrams showing the different isospin operators that contribute to a final $N\Sigma$ state.

The matrix elements for these operators can be easily obtained. Explicit calculations are included in section B, and here only the final results are given. The connection between $\frac{3}{2}$ and $\frac{1}{2}$ isospin states is given by:

$$T^1_{\frac{3}{2}\frac{1}{2}} = \begin{pmatrix} 0 & 0 & -\frac{1}{\sqrt{3}} & 0 \\ 0 & 0 & 0 & -1 \end{pmatrix} \quad T^0_{\frac{3}{2}\frac{1}{2}} = \begin{pmatrix} 0 & \sqrt{\frac{2}{3}} & 0 & 0 \\ 0 & 0 & \sqrt{\frac{2}{3}} & 0 \end{pmatrix} \quad T^{-1}_{\frac{3}{2}\frac{1}{2}} = \begin{pmatrix} -1 & 0 & 0 & 0 \\ 0 & \frac{1}{\sqrt{3}} & 0 & 0 \end{pmatrix}, \qquad (45)$$

while $\vec{\tau}$ matrices connect $\frac{1}{2}$ states:

$$\tau^1_{\frac{1}{2}\frac{1}{2}} = \begin{pmatrix} 0 & \sqrt{2} \\ 0 & 0 \end{pmatrix} \quad \tau^{-1}_{\frac{1}{2}\frac{1}{2}} = \begin{pmatrix} 0 & 0 \\ \sqrt{2} & 0 \end{pmatrix} \quad \tau^0_{\frac{1}{2}\frac{1}{2}} = \begin{pmatrix} 1 & 0 \\ 0 & -1 \end{pmatrix}. \qquad (46)$$

Using the relations:

$$< 00|T^k|1m > \; = \; (-1)^k < 001 - k|1m >= (-1)^k \delta_{mk}$$
$$< 1m'|T^k|1m > \; = \; \sqrt{2} < 1m'|1m1k > \; , \tag{47}$$

we get the corresponding matrix elements for $1 \rightarrow 0$ and $1 \rightarrow 1$ transitions:

$$T^1_{10} = \begin{pmatrix} -1 & 0 & 0 \end{pmatrix} \; T^0_{10} = \begin{pmatrix} 0 & 1 & 0 \end{pmatrix} \; T^{-1}_{10} = \begin{pmatrix} 0 & 0 & -1 \end{pmatrix} \tag{48}$$

$$T^1_{11} = \begin{pmatrix} 0 & -1 & 0 \\ 0 & 0 & -1 \\ 0 & 0 & 0 \end{pmatrix} \; T^0_{11} = \begin{pmatrix} 1 & 0 & 0 \\ 0 & 0 & 0 \\ 0 & 0 & -1 \end{pmatrix} \; T^{-1}_{11} = \begin{pmatrix} 0 & 0 & 0 \\ 1 & 0 & 0 \\ 0 & 1 & 0 \end{pmatrix}. \tag{49}$$

In our work we consider the exchange of only two pseudoscalar mesons. When dealing with isoscalar mesons (η), the only operator that will contribute to the transition will be $\hat{I}_1 \hat{I}_2$, so the matrix element will follow the structure:

$$g_1 < \frac{1}{2} t_{Nf} | \hat{I}_1 \cdot \hat{I}_2 | \frac{1}{2} t >< \frac{1}{2} t | 1 t_1, \frac{1}{2} - \frac{1}{2} >, \tag{50}$$

because the strong vertex will conserve all quantum numbers of the hyperons involved. The Clebsch-Gordan restricts the expression to Σ^0 and Σ^- being the only ones that leads to a non-zero result. The contributions to the $\tilde{T}_0 = 1/2$ and $\tilde{T}_0 = 3/2$ states, given by the product of strong and weak coupling constants, are given in Table VII.

Channel	$\tilde{T}_0 = 1/2$	$\tilde{T}_0 = 3/2$
$\Sigma^0 \Sigma^0 \rightarrow n \Sigma^0$	$g^W_{\Sigma^0 n \eta} g^S_{\Sigma^0 \Sigma^0 \eta} \frac{1}{\sqrt{3}}$	0
$\Sigma^+ \Sigma^- \rightarrow p \Sigma^-$	$g^W_{\Sigma^+ p \eta} g^S_{\Sigma^- \Sigma^- \eta} \sqrt{\frac{2}{3}}$	0

Table VII: Product of weak and strong coupling constants that contribute to the weak transitions when the initial isospurion state takes the values $\tilde{T}_0 = 1/2$ and $\tilde{T}_0 = 3/2$, for the exchange of a η meson.

Now let's concentrate on the π mesons. We must differentiate between two cases. The first one will take place when our weak vertex starts with Σ^-. The coupling of this hyperon with the isospurion leads us to only one final isospin possibility: $\tilde{T} = \frac{3}{2}$, $\tilde{t} = -\frac{1}{2}$. This will restrict our initial expression again. In this case the unique operator allowed is the $\vec{T}_1 \vec{T}_2$:

$$g_2 < \frac{1}{2}t_{Nf}Tt_y|\vec{T}_1 \cdot \vec{T}_2|\frac{3}{2}tT_2t_2 >< \frac{3}{2}t|1t_1, \frac{1}{2} - \frac{1}{2} >, \tag{51}$$

Here, we are dealing with two different final states (Λ and Σ^0), both with an n, calculated in Table VIII. Finally, we face the other two initial possibilities (Σ^+ and Σ^0). For both cases we have:

$$\begin{aligned} g_2 &< \frac{1}{2}t_{Nf}, Tt_Y|\vec{T}_1 \cdot \vec{T}_2|\frac{3}{2}t, T_2t_2 >< \frac{3}{2}t|1t_1, \frac{1}{2} - \frac{1}{2} > + \\ + \; g_3 &< \frac{1}{2}t_{Nf}, Tt_Y|\vec{\tau}_1\vec{\tau}_2|\frac{1}{2}t, T_2t_2 >< \frac{1}{2}t|1t_1, \frac{1}{2} - \frac{1}{2} > . \end{aligned} \tag{52}$$

These are the cases when the initial spurion state can take the value $\tilde{T} = 3/2$. All the final values are also given in Table VIII. As we can see, the coupling constants for the $\Sigma^0\Sigma^0 \rightarrow \Sigma^0 n$ transition are equal to 0. This is due to the Clebsch-Gordan factor $< 10|\vec{T}_2|10 >= \sqrt{2} < 10|101k >= 0$.

Channel	$\tilde{T}_0 = 1/2$	$\tilde{T}_0 = 3/2$
$\Sigma^0\Sigma^0 \rightarrow \Lambda n$	$g^W_{\Sigma^0 n\pi^0} g^S_{\Sigma^0 \Lambda\pi^0}(2/3)$	$g^W_{\Sigma^0 n\pi^0} g^S_{\Sigma^0 \Lambda\pi^0}\left(-\frac{1}{\sqrt{3}}\right)$
$\Sigma^0\Sigma^0 \rightarrow \Sigma^- p$	$g^W_{\Sigma^0 p\pi^-} g^S_{\Sigma^0 \Sigma^-\pi^-}\left(-\frac{\sqrt{2}}{3}\right)$	$g^W_{\Sigma^0 p\pi^-} g^S_{\Sigma^0 \Sigma^-\pi^-}\left(-\sqrt{\frac{2}{3}}\right)$
$\Sigma^0\Sigma^0 \rightarrow \Sigma^0 n$	0	0
$\Sigma^+\Sigma^- \rightarrow \Sigma^- p$	$g^W_{\Sigma^+ p\pi^0} g^S_{\Sigma^- \Sigma^-\pi^0}\left(-\frac{1}{3\sqrt{2}}\right)$	$g^W_{\Sigma^+ p\pi^0} g^S_{\Sigma^- \Sigma^-\pi^0}\left(-\sqrt{\frac{2}{3}}\right)$
$\Sigma^+\Sigma^- \rightarrow \Lambda n$	$g^W_{\Sigma^+ n\pi^+} g^S_{\Sigma^- \Lambda\pi^+}(-1/3)$ $-g^W_{\Sigma^- n\pi^-} g^S_{\Sigma^+ \Lambda\pi^-}$	$g^W_{\Sigma^+ n\pi^+} g^S_{\Sigma^- \Lambda\pi^+}\left(\frac{2}{\sqrt{3}}\right)$
$\Sigma^+\Sigma^- \rightarrow \Sigma^0 n$	$g^W_{\Sigma^+ n\pi^+} g^S_{\Sigma^- \Sigma^0\pi^+}\left(-\frac{1}{3}\right)$ $+g^W_{\Sigma^- n\pi^-} g^S_{\Sigma^+ \Sigma^0\pi^-}$	$g^W_{\Sigma^+ n\pi^+} g^S_{\Sigma^- \Sigma^0\pi^+}\left(\sqrt{\frac{2}{3}}\right)$

Table VIII: Product of weak and strong coupling constants that contribute to the weak transitions when the initial isospurion state takes the values $\tilde{T}_0 = 1/2$ and $\tilde{T}_0 = 3/2$, for the exchange of a π meson.

An explicit computation is given in Apendix (C 4), as well as the special case $\Sigma^0\Sigma^0 \rightarrow \Sigma^0 n$.

E. Spin dependence

As we have previously said, our initial wave function is $^1S_0$. This means that we start with $S = 0$. The possible final spin values in the coupled basis are $S = 0, 1$. Because our quantum number J must be always conserved, our two possibilities for the final wave function are $^1S_0$ and $^3P_0$, as represented in Table IX.

	$\Sigma\Sigma$		YN
Central	$^1S_0$	$\rightarrow$	$^1S_0$
PV	$^1S_0$	$\rightarrow$	$^3P_0$

Table IX: Initial ($\Sigma\Sigma$) and final (YN) partial waves connected through the weak potential.

From the results obtained in Section III B for the transition potential involving the exchange of pseudoscalar mesons, one can see that the operator that can connect the initial and final $^1S_0$ states is the one appearing in the central spin dependent piece $\vec{\sigma}_1 \cdot \vec{\sigma}_2$, while the one that transforms our initial wave function to the $^3P_0$ state is the parity-violating one $\vec{\sigma} \cdot \hat{r}$. Note that, even though we also obtain a tensor operator in our derivation of the potential, this operator carries two units of spin and angular momentum and cannot connect singlet states, and therefore, it does not contribute to our matrix elements.

Let us start with the computation of the matrix element corresponding to the parity violating operator:

$$\hat{O} = \vec{\sigma}_2 \cdot \hat{r} \tag{53}$$

$$
\begin{aligned}
< SM_S|\vec{\sigma}_2 \cdot \hat{r}|S_0 M_{S0} > &= \sum_{m_1 m_2} \sum_{m_{10} m_{20}} < SM_S|\frac{1}{2}m_1\frac{1}{2}m_2 > \\
&\times < \frac{1}{2}m_1\frac{1}{2}m_2|\vec{\sigma}_2 \cdot \hat{r}|\frac{1}{2}m_{10}\frac{1}{2}m_{20} >< \frac{1}{2}m_{10}\frac{1}{2}m_{20}|S_0 M_{S0} > \\
&= \sum_{m_1 m_2} \sum_{m_{10} m_{20}} < SM_S|\frac{1}{2}m_1\frac{1}{2}m_2 >< \frac{1}{2}m_{10}\frac{1}{2}m_{20}|S_0 M_{S0} > \\
&\times < \frac{1}{2}m_2|\vec{\sigma}_2 \cdot \hat{r}|\frac{1}{2}m_{20} >< \frac{1}{2}m_1|\frac{1}{2}m_{10} > .
\end{aligned}
\tag{54}
$$

Using again the Wigner-Eckart theorem [17]:

$$< jm|T_q^k|j'm' >= \frac{(-1)^{2k} < j'm'kq|jm >< j|T^k|j' >}{\sqrt{2j+1}}, \tag{55}$$

with $< \frac{1}{2}|\sigma_2|\frac{1}{2} >=< \frac{1}{2}|2S|\frac{1}{2} >= 2\sqrt{3/2} = \sqrt{6}$ being the reduced matrix element, and using the relations: $\vec{A} \cdot \vec{B} = \sum_\mu (-1)^\mu A^\mu B_{-\mu}$ and $\hat{r}_\mu = \sqrt{\frac{4\pi}{3}}\hat{r}Y_{1\mu}$, we obtain:

$$
\begin{aligned}
< SM_S|\sigma_2 \cdot \hat{r}|S_0 M_{S0} > \; = \; & \sum_{m_1 m_2} \sum_{m_{10} m_{20}} < SM_S|\tfrac{1}{2}m_1 \tfrac{1}{2}m_2 >< \tfrac{1}{2}m_{10}\tfrac{1}{2}m_{20}|S_0 M_{S0} > \\
\times \; & \delta_{m_1 m_{10}} \sum_\mu (-1)^\mu < \tfrac{1}{2}m_{20}1-\mu|\tfrac{1}{2}m_2 > \frac{<\tfrac{1}{2}|\vec{\sigma}_2|\tfrac{1}{2}>}{\sqrt{2}} \sqrt{\frac{4\pi}{3}} Y_{1\mu}(\hat{r}) = \\
= \; & \sum_{m_1 m_2} \sum_{m_{10} m_{20}} < SM_S|\tfrac{1}{2}m_1 \tfrac{1}{2}m_2 >< \tfrac{1}{2}m_{10}\tfrac{1}{2}m_{20}|S_0 M_{S0} > \\
\times \; & \delta_{m_1 m_{10}} \sum_\mu (-1)^\mu < \tfrac{1}{2}m_{20}1-\mu|\tfrac{1}{2}m_2 > \sqrt{3}\sqrt{\frac{4\pi}{3}} Y_{1\mu}(\hat{r}).
\end{aligned}
\tag{56}
$$

To simplify the sums we can do some algebra taking in account that M_S and M_{S0} are fixed and that a $\delta_{m_1 m_{10}}$ appears due to the $< \tfrac{1}{2}m_1 \tfrac{1}{2}m_2|\vec{\sigma}_2 \cdot \hat{r}|\tfrac{1}{2}m_{10}\tfrac{1}{2}m_{20} >$ term in Eq.(54):

$$
M_S = m_1 + m_2, \qquad M_{S0} = m_{10} + m_{20}, \qquad m_2 = m_{20} - \mu.
\tag{57}
$$

Combining these relations one can express the quantum numbers as a function of m_{10}, M_{S0} and M_S:

$$
\mu = M_{S0} - M_S, \qquad m_{20} = M_{S0} - m_{10}, \qquad m_2 = M_S - m_{10}, \qquad m_1 = m_{10}.
\tag{58}
$$

leading to a final expression for the PV spin matrix element:

$$
\begin{aligned}
< SM_S|\vec{\sigma}_2 \cdot \hat{r}|S_0 M_{S0} > \; = \; & \sum_{m_{10}} < SM_S|\tfrac{1}{2}m_{10}\tfrac{1}{2}(M_S - m_{10}) >< \tfrac{1}{2}m_{10}\tfrac{1}{2}(M_{S0} - m_{10})|S_0 M_{S0} > \\
\times \; & (-1)^{M_{S0}-M_S}\sqrt{3} < \tfrac{1}{2}(M_{S0}-m_{10})1(M_S - M_{S0})|\tfrac{1}{2}(M_S - m_{10}) > \\
\times \; & \sqrt{\frac{4\pi}{3}} Y_{1(M_S - M_{S0})}(\hat{r}).
\end{aligned}
\tag{59}
$$

Further simplifications can be performed knowing that the radial integration (as we will see later) imposes the constraints: $S_0 = M_{S0} = 0$ and $S = 1$:

$$
\begin{aligned}
< 1M_S|\vec{\sigma}_2 \cdot \hat{r}|00 > \; = \; & \sum_{m_{10}} < 1M_S|\tfrac{1}{2}m_{10}\tfrac{1}{2}(M_S - m_{10}) >< \tfrac{1}{2}m_{10}\tfrac{1}{2}-m_{10}|00 > \\
\times \; & (-1)^{-M_S}\sqrt{3} < \tfrac{1}{2}(-m_{10})1M_S|\tfrac{1}{2}(M_S - m_{10}) > \sqrt{\frac{4\pi}{3}} Y_{1M_S}(\hat{r}).
\end{aligned}
\tag{60}
$$

The second and last spin operator is the central one:

$$
\hat{O} = \vec{\sigma}_1 \cdot \vec{\sigma}_2 \,,
\tag{61}
$$

which can be easily evaluated knowing that:

$$
\begin{aligned}
\vec{S} \; = \; & \vec{S}_1 + \vec{S}_2 = \frac{1}{2}(\vec{\sigma}_1 + \vec{\sigma}_2) \\
\vec{\sigma}_1 \cdot \vec{\sigma}_2 \; = \; & 2\vec{S}^2 - \vec{\sigma}_1^2/2 - \vec{\sigma}_2^2/2 = 2\vec{S}^2 - 2\vec{S}_1^2 - 2\vec{S}_2^2.
\end{aligned}
\tag{62}
$$

Therefore,

$$< SM_S|\vec{\sigma}_1 \cdot \vec{\sigma}_2|S_0 M_{S0} >=< SM_S|2\vec{S}^2 - 2\vec{S}_1^2 - 2\vec{S}_2^2|S_0 M_{S0} >=$$

$$= 2 < SM_S||S_0 M_{S0} > [S(S+1) - 3/2] = \delta_{SS_0}\delta_{M_S M_{S0}}2[S(S+1) - 3/2].$$

(63)

Since $S_0 = 0$ (and thus $S = 0$) the numerical value for the corresponding matrix element is:

$$< 00|\vec{\sigma}_1 \cdot \vec{\sigma}_2|00 >= 2[S(S+1) - 3/2] = -3.$$

(64)

IV.   Discussion of results

	$(\Lambda\Lambda - \Lambda\Lambda) \to \Lambda n$	$(\Lambda\Lambda - \Lambda\Lambda) \to \Sigma^0 n$	$(\Lambda\Lambda - \Lambda\Lambda) \to \Sigma^- p$	$\Gamma_{\Lambda\Lambda}$
π	0.1350	2.3824	4.7648	7.2822
η	0.8945	0.2557×10^{-3}	0.5114×10^{-3}	0.8953
$\pi + \eta$	1.2983	2.3526	4.7052	8.3560
	$(\Lambda\Lambda - \Xi N) \to \Lambda n$	$(\Lambda\Lambda - \Xi N) \to \Sigma^0 n$	$(\Lambda\Lambda - \Xi N) \to \Sigma^- p$	$\Gamma_{\Xi N}$
π	0.8274	0.7726	1.5451	1.6015
η	0.25486	0.05339	0.1068	0.4151
$\pi + \eta$	1.9892	1.2320	2.4639	5.6851
	$(\Lambda\Lambda - \Sigma\Sigma) \to \Lambda n$	$(\Lambda\Lambda - \Sigma\Sigma) \to \Sigma^0 n$	$(\Lambda\Lambda - \Sigma\Sigma) \to \Sigma^- p$	$\Gamma_{\Sigma\Sigma}$
π	0.1862	0.1281	0.2563	0.5706
η	0.2123	0.0534	0.1068	0.3725
$\pi + \eta$	0.07772	0.2001	0.4003	0.6781
	$\Lambda\Lambda \to \Lambda n$	$\Lambda\Lambda \to \Sigma^0 n$	$\Lambda\Lambda \to \Sigma^- p$	$\Gamma_{\pi+\eta}$
π	1.7746	3.0415	6.0831	10.8992
η	0.9643	0.4015×10^{-3}	0.8030×10^{-3}	0.9655
$\pi + \eta$	5.3129	2.9921	5.9842	14.2893

Table X: In the first row we show the results obtained for the weak decay of $^6_{\Lambda\Lambda}$He when only the diagonal term of the initial $\Lambda\Lambda$ wave function, $(\Lambda\Lambda - \Lambda\Lambda)$, is considered Ref.[18]. In the second row: when only the $(\Lambda\Lambda - \Xi N)$ component is considered Ref.[18]. In the third one the new results obtained in this work are shown considering only the $(\Lambda\Lambda - \Sigma\Sigma)$ component. In the fourth row the combined results considering the three components of the initial wave function are presented. All results have been obtained exchanging a π, a η ans the combination of both. All the values are given in units of $\times 10^{-3}\Gamma_\Lambda$ with $\Gamma_\Lambda = 3.8 \times 10^9 s^{-1}$ the decay rate of a Λ in free space.

	$\Gamma(\Lambda\Lambda - \Lambda\Lambda)$	$\Gamma(\Lambda\Lambda - \Xi N)$	$\Gamma(\Lambda\Lambda - \Sigma\Sigma)$
π	0.02	0.36	0.48
η	1166.01	1.59	1.33
$\pi + \eta$	0.19	0.54	0.13

Table XI: $\Lambda n / \Sigma N$ ratio for the three wave function components and for the two mesons involved.

	$\Gamma(\Lambda\Lambda - \Lambda\Lambda)$	$\Gamma(\Lambda\Lambda - \Xi N)$	$\Gamma(\Lambda\Lambda - \Sigma\Sigma)$
π	3.96	3.35	0.02
η	0.02	6.42×10^{-4}	6.25×10^{-3}
$\pi + \eta$	2.37	1.66	0.01

Table XII: PV/PC contributions ratio for the three wave function components and for the exchange of π, η and both.

In this section the results from all the previous computations are presented. This is an exploratory study of the contribution of the π and η mesons to the decay rate produced by the $\Lambda\Lambda - \Sigma\Sigma$ component. All of the results are computed in a previously on Refs. [10, 12].

As it can be seen on the results, the transition rate for $\Sigma^0 n$ and $\Sigma^- p$ differs only by a factor 2. This is due to the fact that they have the same final state structure except for the Clebsch-Gordan coefficient for the spin. For $\Sigma^0 n$ the Clebsch-Gordan is $\frac{1}{\sqrt{3}}$, while for $\Sigma^- p$ is $\sqrt{\frac{2}{3}}$. Since we are dealing with a transition amplitude, all this values are squared, leading to this factor 2.

Regarding the contribution of each pseudoscalar to the final decay rate, the η exchange is negligible as compared to the pion exchange. For the $(\Lambda\Lambda - \Lambda\Lambda)$ value it represents a $10, 71\%$ of the total contribution and similar values are obtained for $(\Lambda\Lambda - \Xi N)$ which is a $7, 3\%$, and also for the total contribution which leads to a $6, 75\%$. For the case $(\Lambda\Lambda - \Sigma\Sigma)$ the exchange of η contributes in a $54, 9\%$ and cannot be neglected. Also the η meson exchange has a remarkable role in the Λn final state in all cases, specially in the $(\Lambda\Lambda - \Lambda\Lambda)$ channel. For the pions and also for the contribution of both, the ΣN final state has a larger decay rate, as it can be seen in Table (X).

If we compute the PV/PC ratio, as displayed in table (ref), it is easy to see the leading contribution for each meson. In all channels except $(\Lambda\Lambda - \Sigma\Sigma)$, the largest contribution to PV comes from the π exchange up to a 5 factor, while for the η meson exchange, the contribution to PC can be up to three orders of magnitude bigger than PV. When the two exchanges are taken into account, the ratio balances again in favour of PV. For the $(\Lambda\Lambda - \Sigma\Sigma)$ channel, the exchange of a π, an η as well as the combination of both exchanges contributes more significantly to the PC term.

As we can see in Table (X), the role played by $\Lambda\Lambda - \Sigma\Sigma$ component of the wave function is not very significant at the level of the total rate, being one order of magnitude below to the corresponding $\Gamma_{\Lambda\Lambda}$ and $\Gamma_{\Xi N}$. Regarding the rates of the $(\Lambda\Lambda - \Lambda\Lambda) \to \Lambda n$, the sum of both contributions is constructive when leading to final Λn state while is slightly destructive when dealing with $(\Lambda\Lambda - \Sigma N)$ states. On the contrary, the $\Lambda\Lambda - \Xi N$ component of the of the wave function shows a constructive interference for all final states. The behaviour we obtained for the $\Lambda\Lambda - \Sigma\Sigma$ contribution is similar to the one shown for the $\Lambda\Lambda - \Lambda\Lambda$ one.

It is difficult to reconcile this numbers with what we see from Fig. (1) since we would expect much more similar values for $\Gamma_{\Sigma\Sigma}$ and $\Gamma_{\Xi N}$, and much more difference between these rates and $\Gamma_{\Lambda\Lambda}$.

Our calculations of the decay rates have been based on the exchange of π and η. In order to have a complete picture of the contribution of the $\Sigma\Sigma - YN$ transitions to the decay of $^{6}_{\Lambda\Lambda}\text{He}$, we need to incorporate the exchange of not only π and η, but also K and vector mesons, such as ρ, ω and K^{*}. This is out of the scope of the present thesis and will be addressed in a future work.

Appendices

A.   r-space integrals

In this section we compute $\sum_{SM_S} | < \vec{k}, SM_S|\hat{O}|\psi^{REL}, S_0 = 0\, M_{S0} = 0 > |^2 = | < \psi_{YN}^{1S_0}(\vec{k},\vec{r})|\hat{O}|\psi_{\Sigma\Sigma}^{1S_0}(\vec{r}) > |^2$ appearing in Eq. (8). We calculate separately the terms for $S = 1$ and for $S = 0$, taking in account the results from the previous section. To illustrate the calculation, we take for the initial wavefunctions harmonic oscillator wavefunctions, while for the outgoing ones take plane waves. Nevertheless, the final result has been computed using the correlated wave functions obtained solving the appropriate G-matrix and T-matrix equations.

$$\psi_{\Sigma\Sigma}^{1S_0}(\vec{r}) = \sqrt{\frac{4}{\sqrt{\pi}b^3}}e^{-r^2/2b^2}Y_{00}(\hat{r})$$

$$\psi_{YN}^{1S_0}(\vec{k},\vec{r}) = e^{i\vec{k}\cdot\vec{r}} = \sum_{LM_L} 4\pi i^L j_L(kr,r)Y_{LM_L}^*(\hat{k}r)Y_{LM_L}(\hat{r}), \tag{A1}$$

with b a parameter of the plane wave functions.

For $S = 0$, the spin-dependent term, we have:

$$< \psi_{YN}^{1S_0}(\vec{k},\vec{r})|\hat{O}|\psi_{\Sigma\Sigma}^{1S_0}(\vec{r}) >=$$

$$= \frac{1}{(2\pi)^{3/2}} \int d^3r \psi_f^{REL} V_{SS}(\vec{r})\psi_0^{REL} < S = 0\, M_S = 0|\vec{\sigma}_1\cdot\vec{\sigma}_2|S_0 = 0\, M_{S0} = 0 >= \tag{A2}$$

$$= \frac{1}{(2\pi)^{3/2}} \int d^3r \psi_f^{REL} V_{SS}(\vec{r})\psi_0^{REL}(-3).$$

Where we know from Eq. (24):

$$V_{SS} = G_W^2 g_S \frac{B}{2\bar{M}2M}\frac{1}{3}\left(\frac{e^{-mr}}{2\pi r}m^2\right) = V_S'\frac{e^{-mr}}{2\pi r} \tag{A3}$$

$$< \psi_{YN}^{1S_0}(\vec{k},\vec{r})|\ \hat{O}\ |\psi_{\Sigma\Sigma}^{1S_0}(\vec{r}) >=$$

$$= \frac{1}{(2\pi)^{3/2}} \int dr r^2 \int d\hat{r} \left[\sum_{LM_L} 4\pi i^L j_L(kr)Y_{LM_L}^*(\hat{k})Y_{LM_L}(\hat{r})\right]$$

$$\times \left[G_W^2 g_S \frac{B}{2\bar{M}2M}\frac{1}{3}\left(\frac{e^{-mr}}{2\pi r}m^2\right)\right]\left[\frac{2}{\pi^{1/4}b^{3/2}}e^{-r^2/2b^2}Y_{00}(\hat{r})\right](-3). \tag{A4}$$

Integrating the terms depending on $\hat{r}$:

$$\int d\hat{r} Y_{LM_L}(\hat{r})Y_{00}(\hat{r}) = \frac{1}{\sqrt{4\pi}}\delta_{L0}\delta_{M_L0}, \tag{A5}$$

So our integral becomes:

$$< \psi_{YN}^{^1S_0}(\vec{k},\vec{r})| \ \hat{O} \ |\psi_{\Sigma\Sigma}^{S}(\vec{r}) >=$$

$$= -\frac{1}{(4\pi)^{5/4}}Y_{00}^*(\hat{k})G_W^2 g_S \frac{B}{\bar{M}M}\frac{m^2}{b^{3/2}}\int dr r^2 j_0(kr)\frac{e^{-mr}}{r}e^{-r^2/2b^2} =$$

$$= -\frac{1}{(4\pi)^{5/4}}Y_{00}^*(\hat{k})G_W^2 g_S \frac{B}{\bar{M}M}\frac{m^2}{b^{3/2}}\int dr r^2 \left[\frac{sin(kr)}{kr}\right]\frac{e^{-mr}}{r}e^{-r^2/2b^2} =$$

$$= -\frac{1}{(4\pi)^{5/4}}Y_{00}^*(\hat{k})G_W^2 g_S \frac{B}{\bar{M}M}\frac{m^2}{b^{3/2}}\int dr \left[\frac{sin(kr)}{k}\right]e^{-mr}e^{-r^2/2b^2}. \tag{A6}$$

For $S=1$ we take again from Eq. (24):

$$V_{PV}(r) = G_W^2 g_S \frac{A}{2M}m\frac{e^{-mr}}{4i\pi r}\left(1+\frac{m}{r}\right) \tag{A7}$$

$$< \psi_{YN}^{^3P_0}(\vec{k},\vec{r})|\hat{O}|\psi_{\Sigma\Sigma}^{^1S_0}(\vec{r}) >=$$

$$= \frac{1}{(2\pi)^{3/2}}\int d^3r \psi_f^{REL} * V_{PV}(\vec{r})\psi_0^{REL} < 1M_S|\vec{\sigma}_2\cdot\vec{r}|S_0 = 0 \, M_{S0} = 0 >=$$

$$= \frac{1}{(2\pi)^{3/2}}\int dr r^2 \int d\hat{r}\left[\sum_{LM_L}4\pi i^L j_L(kr)Y_{LM_L}^*(\hat{k})Y_{LM_L}(\hat{r})\right]\left[G_W^2 g_S \frac{Am}{2M}\frac{e^{-mr}}{4i\pi r}\left(1+\frac{m}{r}\right)\right]$$

$$\times \left[\frac{2}{\pi^{1/4}b^{3/2}}e^{-r^2/2b^2}Y_{00}(\hat{r})\right] < 1M_S|\vec{\sigma}_2\cdot\vec{r}|S_0 = 0 \, M_{S0} = 0 >=$$

$$= \frac{1}{(2\pi)^{3/2}}\int dr r^2 \int d\hat{r}\left[\sum_{LM_L}4\pi i^L j_L(kr)Y_{LM_L}^*(\hat{k})Y_{LM_L}(\hat{r})\right]$$

$$\times \left[G_W^2 g_S \frac{Am}{2M}\frac{e^{-mr}}{4i\pi r}\left(1+\frac{m}{r}\right)\right]\left[\frac{2}{\pi^{1/4}b^{3/2}}e^{-r^2/2b^2}Y_{00}(\hat{r})\right]$$

$$\times \left[\sum_{m_{10}} < 1M_S|\frac{1}{2}m_{10}\frac{1}{2}(M_S - m_{10}) >< \frac{1}{2}m_{10}\frac{1}{2} - m_{10}|S_0 = 0 \, M_{S0} = 0 >\right.$$

$$\times \ (-1)^{-M_S}\sqrt{3} < \frac{1}{2}(-m_{10})1M_S|\frac{1}{2}(M_S - m_{10}) > \sqrt{\frac{4\pi}{3}}Y_{1M_S}(\hat{r})\right]. \tag{A8}$$

Performing the $\int d\hat{r}$ integral as we did before:

$$\int d\hat{r}Y_{LM_L}(\hat{r})Y_{00}(\hat{r})Y_{1M_S}(\hat{r}) = \frac{1}{\sqrt{4\pi}}\int d\hat{r}Y_{LM_L}(\hat{r})Y_{1M_S}(\hat{r}) = \frac{1}{\sqrt{4\pi}}\delta_{L1}\delta_{M_L M_S}, \tag{A9}$$

we can simplify our expression:

$$< \psi_{YN}^{^3P_0}(\vec{k},\vec{r})| \quad \hat{O} \quad |\psi_{\Sigma\Sigma}^{^1S_0}(\vec{r}) >=$$

$$= \frac{1}{(2\pi)^{3/2}} Y_{LM_L}^*(\hat{k}) G_W^2 g_S \frac{Am}{M} \frac{(-1)^{M_S}}{\pi^{1/4}b^{3/2}}$$

$$\times \left(\sum_{m_{10}} < 1M_S|\frac{1}{2}m_{10}\frac{1}{2}(M_S-m_{10}) >< \frac{1}{2}m_{10}\frac{1}{2}-m_{10}|S_0=0\,M_{S0}=0 > \right.$$

$$\times \left. < \frac{1}{2}(-m_{10})1M_S|\frac{1}{2}(M_S-m_{10}) > \right) \int dr r^2 j_1(kr) \frac{e^{-mr}}{r} e^{-r^2/2b^2} \left(1+\frac{m}{r} \right) =$$

$$= \frac{1}{(2\pi)^{3/2}} Y_{LM_L}^*(\hat{k}) G_W^2 g_S \frac{Am}{M} \frac{(-1)^{M_S}}{\pi^{1/4}b^{3/2}} \left(\sum_{m_{10}} < 1M_S|\frac{1}{2}m_{10}\frac{1}{2}(M_S-m_{10}) > \right.$$

$$\times \left. < \frac{1}{2}m_{10}\frac{1}{2}-m_{10}|S_0=0\,M_{S0}=0 >< \frac{1}{2}(-m_{10})1M_S|\frac{1}{2}(M_S-m_{10}) > \right)$$

$$\times \int dr \left(\frac{sin(kr)}{k^2r} - cos(kr) \right) e^{-mr} e^{-r^2/2b^2} \left(1+\frac{m}{r} \right). \tag{A10}$$

B. Isospin matrix elements

In this section we work with the isospin part of our decay rate expression:

$$< \frac{1}{2} - \frac{1}{2}|\hat{O}(T)|\frac{1}{2} - \frac{1}{2} >=$$

$$=< \frac{1}{2} - \frac{1}{2}|T_{10}t_{10}T_{20}t_{20} >< T_{10}t_{10}T_{20}t_{20}|\hat{O}(T)|T_1t_1T_2t_2 >< T_1t_1T_2t_2|\frac{1}{2} - \frac{1}{2} > . \tag{B1}$$

For that, we need to know the reduced matrix elements of the operators themselves. In this section, we are using the Wigner-Eckart theorem (Eq. 55):

$$< jm|T_q^k|j'm' >= \frac{(-1)^{2k} < j'm'kq|jm >< j|T^k|j' >}{\sqrt{2j+1}}, \tag{B2}$$

to get rid of m dependence.

To calculate $< j|T^k|j' >$ we are going to use two properties. The first one will be the relation between cartesian and spherical components:

$$< \frac{3}{2}m_A|\vec{\tau}_{AN}|\frac{1}{2}m_N >=< \frac{1}{2}m_N 1 - 1|\frac{3}{2}m_A > \frac{1}{\sqrt{2}} \begin{pmatrix} 1 \\ i \\ 0 \end{pmatrix} +$$

$$+ < \frac{1}{2}m_N 10|\frac{3}{2}m_A > \begin{pmatrix} 0 \\ 0 \\ 1 \end{pmatrix} + < \frac{1}{2}m_N 11|\frac{3}{2}m_A > \left(-\frac{1}{\sqrt{2}}\right) \begin{pmatrix} 1 \\ -i \\ 0 \end{pmatrix}, \tag{B3}$$

so:

$$< \frac{3}{2}m_A|\tau^x|\frac{1}{2}m_N > = \frac{1}{\sqrt{2}}(< \frac{1}{2}m_N 1 - 1|\frac{3}{2}m_A > - < \frac{1}{2}m_N 11|\frac{3}{2}m_A >)$$

$$< \frac{3}{2}m_A|\tau^z|\frac{1}{2}m_N > = < \frac{1}{2}m_N 10|\frac{3}{2}m_A >$$

$$< \frac{3}{2}m_A|\tau^y|\frac{1}{2}m_N > = \frac{i}{\sqrt{2}}(< \frac{1}{2}m_N 1 - 1|\frac{3}{2}m_A > + < \frac{1}{2}m_N 11|\frac{3}{2}m_A >). \tag{B4}$$

With this, we can express it in spherical components:

$$\tau^1 = -\frac{1}{\sqrt{2}}(\tau^x + i\tau^y) =< \frac{1}{2}m_N 11|\frac{3}{2}m_A >=< \frac{3}{2}m_A|\tau^1|\frac{1}{2}m_N >$$

$$\tau^0 = \tau^z =< \frac{1}{2}m_N 10|\frac{3}{2}m_A >=< \frac{3}{2}m_A|\tau^0|\frac{1}{2}m_N >$$

$$\tau^{-1} = \frac{1}{\sqrt{2}}(\tau^x - i\tau^y) < \frac{1}{2}m_N 1 - 1|\frac{3}{2}m_A >=< \frac{3}{2}m_A|\tau^{-1}|\frac{1}{2}m_N > . \tag{B5}$$

The second property comes from the Wigner-Eckart theorem mentioned previously:

$$< \frac{3}{2}m_A|\tau^0|\frac{1}{2}m_N >= \frac{(-1)^{2\cdot 0} < \frac{1}{2}m_N 10|\frac{3}{2}m_A >< \frac{3}{2}||\tau|\frac{1}{2} >}{2}. \tag{B6}$$

Combining these two expressions we get:

$$< \frac{1}{2}m_N 10|\frac{3}{2}m_A > = \frac{(-1)^{2\cdot 0} < \frac{1}{2}m_N 10|\frac{3}{2}m_A >< \frac{3}{2}||\tau|\frac{1}{2} >}{2} \tag{B7}$$

$$< \frac{3}{2}||\tau|\frac{1}{2} > = 2. \tag{B8}$$

Due to the fact that the reduced matrix elements do not depend on the projection values for the isospin, it can be obtained with all other projections, leading to the same exact result.

For the reduced matrix elements involving integer numbers we used [10]:

$$< 00|T^k|1m >= (-1)^k < 001 - k|1m >= (-1)^k \delta_{mk} \tag{B9a}$$

$$< 1m|T^k|00 >= \delta_{mk} \tag{B9b}$$

$$< 1m'|T^k|1m >= \sqrt{2} < 1m'|1m1k > . \tag{B9c}$$

We are now capable of obtaining the matrix for each operator. We are going to compute T, an operator that allows us to connect $T = 3/2$ states and $T = 1/2$ states, and τ that allows us to connect two $T = 1/2$ states.

$$< \frac{1}{2}\frac{1}{2}|T^1|\frac{3}{2} - \frac{1}{2} > = < \frac{3}{2} - \frac{1}{2}11|\frac{1}{2}\frac{1}{2} > (-1)^{2\cdot 1}\frac{1}{\sqrt{2}} < \frac{1}{2}|T^1|\frac{3}{2} >=$$
$$= \frac{1}{\sqrt{6}}(-1)^{2\cdot 1}\frac{1}{\sqrt{2}} < \frac{1}{2}|T^1|\frac{3}{2} >= \frac{1}{\sqrt{6}} \cdot 1 \cdot \frac{1}{\sqrt{2}}(-2) = -\frac{1}{\sqrt{3}}$$
$$< \frac{1}{2} - \frac{1}{2}|T^1|\frac{3}{2} - \frac{3}{2} > = < \frac{3}{2} - \frac{3}{2}11|\frac{1}{2} - \frac{1}{2} > (-1)^{2\cdot 1}\frac{1}{\sqrt{2}} < \frac{1}{2}|T^1|\frac{3}{2} >=$$
$$= \frac{1}{\sqrt{2}}(-1)^{2\cdot 1}\frac{1}{\sqrt{2}} < \frac{1}{2}|T^1|\frac{3}{2} >= \frac{1}{\sqrt{2}} \cdot 1 \cdot \frac{1}{\sqrt{2}}(-2) = -1 \tag{B10}$$

$$T^1 = \begin{pmatrix} 0 & 0 & -1\sqrt{3} & 0 \\ 0 & 0 & 0 & -1 \end{pmatrix} \tag{B11}$$

$$< \frac{1}{2}\frac{1}{2}|T^0|\frac{3}{2}\frac{1}{2} > = < \frac{3}{2}\frac{1}{2}10|\frac{1}{2}\frac{1}{2} > (-1)^{2\cdot 1}\frac{1}{\sqrt{2}} < \frac{1}{2}|T^0|\frac{3}{2} >=$$
$$= -\frac{1}{\sqrt{3}}(-1)^{2\cdot 1}\frac{1}{\sqrt{2}} < \frac{1}{2}|T^0|\frac{3}{2} >= -\frac{1}{\sqrt{3}} \cdot 1 \cdot \frac{1}{\sqrt{2}}(-2) = \sqrt{\frac{2}{3}}$$
$$< \frac{1}{2} - \frac{1}{2}|T^0|\frac{3}{2} - \frac{1}{2} > = < \frac{3}{2} - \frac{1}{2}10|\frac{1}{2} - \frac{1}{2} > (-1)^{2\cdot 1}\frac{1}{\sqrt{2}} < \frac{1}{2}|T^0|\frac{3}{2} >=$$
$$= \frac{1}{\sqrt{2}}(-1)^{2\cdot 1}\frac{1}{\sqrt{2}} < \frac{1}{2}|T^0|\frac{3}{2} >= \frac{1}{\sqrt{2}} \cdot 1 \cdot \frac{1}{\sqrt{2}}(-2) = \sqrt{\frac{2}{3}} \tag{B12}$$

$$T^0 = \begin{pmatrix} 0 & \sqrt{\frac{2}{3}} & 0 & 0 \\ 0 & 0 & \sqrt{\frac{2}{3}} & 0 \end{pmatrix} \tag{B13}$$

$$<\frac{1}{2}\frac{1}{2}|\mathrm{T}^{-1}|\frac{3}{2}\frac{3}{2}> \; = \; <\frac{3}{2}\frac{3}{2}1-1|\frac{1}{2}\frac{1}{2}> (-1)^{2\cdot 1}\frac{1}{\sqrt{2}} <\frac{1}{2}||\mathrm{T}^{-1}||\frac{3}{2}> =$$
$$= -\frac{1}{\sqrt{2}}(-1)^{2\cdot 1}\frac{1}{\sqrt{2}} <\frac{1}{2}||\mathrm{T}^{-1}||\frac{3}{2}> = -\frac{1}{\sqrt{2}}\cdot 1 \cdot \frac{1}{\sqrt{2}}(-2) = -1$$
$$<\frac{1}{2}-\frac{1}{2}|\mathrm{T}^{-1}|\frac{3}{2}\frac{1}{2}> \; = \; <\frac{3}{2}\frac{1}{2}1-1|\frac{1}{2}-\frac{1}{2}> (-1)^{2\cdot 1}\frac{1}{\sqrt{2}} <\frac{1}{2}||\mathrm{T}^{-1}||\frac{3}{2}> =$$
$$= \frac{1}{\sqrt{6}}(-1)^{2\cdot 1}\frac{1}{\sqrt{2}} <\frac{1}{2}||\mathrm{T}^{-1}||\frac{3}{2}> = -\frac{1}{\sqrt{3}}\cdot 1 \cdot \frac{1}{\sqrt{2}}(-2) = -\frac{1}{\sqrt{3}} \tag{B14}$$

$$T^{-1} = \begin{pmatrix} -1 & 0 & 0 & 0 \\ 0 & \frac{1}{\sqrt{3}} & 0 & 0 \end{pmatrix}. \tag{B15}$$

We can do the same for the transition $\frac{1}{2} \to \frac{1}{2}$ with a τ operator:

$$<\frac{1}{2}-\frac{1}{2}|\tau^1|\frac{1}{2}\frac{1}{2}> \; = \; <\frac{1}{2}\frac{1}{2}11|\frac{1}{2}-\frac{1}{2}> (-1)^{2\cdot 1}\frac{1}{\sqrt{2}} <\frac{1}{2}||\tau^1||\frac{1}{2}> =$$
$$= -\sqrt{\frac{2}{3}}(-1)^{2\cdot 1}\frac{1}{\sqrt{2}} <\frac{1}{2}||\tau^1||\frac{3}{2}> = -\sqrt{\frac{2}{3}}\cdot 1 \cdot \frac{1}{\sqrt{2}}(\sqrt{6}) = -\sqrt{2} \tag{B16}$$

$$\tau^1 = \begin{pmatrix} 0 & \sqrt{2} \\ 0 & 0 \end{pmatrix} \tag{B17}$$

$$<\frac{1}{2}\frac{1}{2}|\tau^{-1}|\frac{1}{2}-\frac{1}{2}> \; = \; <\frac{1}{2}-\frac{1}{2}11|\frac{1}{2}\frac{1}{2}> (-1)^{2\cdot 1}\frac{1}{\sqrt{2}} <\frac{1}{2}||\tau^{-1}||\frac{1}{2}> =$$
$$= \sqrt{\frac{2}{3}}(-1)^{2\cdot 1}\frac{1}{\sqrt{2}} <\frac{1}{2}||\tau^{-1}||\frac{3}{2}> = \sqrt{\frac{2}{3}}\cdot 1 \cdot \frac{1}{\sqrt{2}}(\sqrt{6}) = \sqrt{2} \tag{B18}$$

$$\tau^{-1} = \begin{pmatrix} 0 & 0 \\ \sqrt{2} & 0 \end{pmatrix} \tag{B19}$$

$$<\frac{1}{2}-\frac{1}{2}|\tau^0|\frac{1}{2}-\frac{1}{2}> \; = \; <\frac{1}{2}-\frac{1}{2}11|\frac{1}{2}-\frac{1}{2}> (-1)^{2\cdot 1}\frac{1}{\sqrt{2}} <\frac{1}{2}||\tau^0||\frac{1}{2}> =$$
$$= \frac{1}{\sqrt{3}}(-1)^{2\cdot 1}\frac{1}{\sqrt{2}} <\frac{1}{2}||\tau^0||\frac{3}{2}> = \frac{1}{\sqrt{3}}\cdot 1 \cdot \frac{1}{\sqrt{2}}(\sqrt{6}) = 1$$
$$<\frac{1}{2}\frac{1}{2}|\tau^0|\frac{1}{2}\frac{1}{2}> \; = \; <\frac{1}{2}\frac{1}{2}11|\frac{1}{2}\frac{1}{2}> (-1)^{2\cdot 1}\frac{1}{\sqrt{2}} <\frac{1}{2}||\tau^0||\frac{1}{2}> =$$
$$= -\frac{1}{\sqrt{3}}(-1)^{2\cdot 1}\frac{1}{\sqrt{2}} <\frac{1}{2}||\tau^0||\frac{3}{2}> = -\frac{1}{\sqrt{3}}\cdot 1 \cdot \frac{1}{\sqrt{2}}(\sqrt{6}) = -1 \tag{B20}$$

$$\tau^0 = \begin{pmatrix} 1 & 0 \\ 0 & -1 \end{pmatrix}. \tag{B21}$$

The last step is to obtain each value for the different diagrams we get at the very beginning of this work. The general expression can be obtained combining all the terms obtained before:

$$
\begin{aligned}
< \frac{1}{2} - &\frac{1}{2} |\hat{O}(T)| \frac{1}{2} - \frac{1}{2} >= \\
&= < \frac{1}{2} - \frac{1}{2} |T_{10}t_{10}T_{20}t_{20} >< T_{10}t_{10}T_{20}t_{20}|\hat{O}(T)|T_1t_1T_2t_2 >< T_1t_1T_2t_2|\frac{1}{2} - \frac{1}{2} >= \\
&= < \frac{1}{2} - \frac{1}{2} |T_{10}t_{10}T_{20}t_{20} >< T_{10}t_{10}T_{20}t_{20}|A_1 \cdot A_2|T_1t_1T_2t_2 >< T_1t_1T_2t_2|\frac{1}{2} - \frac{1}{2} >= \\
&= < \frac{1}{2} - \frac{1}{2} |T_{10}t_{10}T_{20}t_{20} >< T_1t_1T_2t_2|\frac{1}{2} - \frac{1}{2} > \sum_{\mu}(-1)^{\mu} \\
&\times \; < T_{10}t_{10}|A_1^{\mu}|T_1t_1 >< T_{20}t_{20}|A_2^{-\mu}|T_2t_2 >, \tag{B22}
\end{aligned}
$$

where here the operator A can be both τ or T depending on the isospin value of initial and final states.

C. Example of calculation of coupling constants

1. Strong example: the $\Sigma^- \pi^+ \to \Sigma^0$ vertex

As an example, the computations for the $\Sigma^- \pi^+ \to \Sigma^0$ vertex strong coupling constant are explicitly written down. As we previously said, only the two last terms of the Lagrangian will contribute to the final value:

$$\frac{D}{2}\text{Tr}[\bar{B}\gamma^\mu\gamma_5\{u_\mu, B\}] + \frac{F}{2}\text{Tr}[\bar{B}\gamma^\mu\gamma_5[u_\mu, B]], \tag{C1}$$

with the particular values for B, $\bar{B}$ and ϕ:

$$B = \begin{pmatrix} 0 & 0 & 0 \\ \Sigma^- & 0 & 0 \\ 0 & 0 & 0 \end{pmatrix} \quad \bar{B} = \begin{pmatrix} \frac{1}{\sqrt{2}}\bar{\Sigma}^0 & 0 & 0 \\ 0 & -\frac{1}{\sqrt{2}}\bar{\Sigma}^0 & 0 \\ 0 & 0 & 0 \end{pmatrix} \quad \phi = \begin{pmatrix} 0 & \pi^+ & 0 \\ 0 & 0 & 0 \\ 0 & 0 & 0 \end{pmatrix}. \tag{C2}$$

The first step is to compute both the commutator and anticommutator for each term we need. Using $u_\mu = i(u^\dagger\partial_\mu u - u\partial_\mu u^\dagger) = \frac{-\sqrt{2}}{f}\partial_\mu\phi$ we get:

$$\{u_\mu, B\} = \frac{-\sqrt{2}}{f}\partial_\mu(\pi^+)\Sigma^- \left[\begin{pmatrix} 0 & 1 & 0 \\ 0 & 0 & 0 \\ 0 & 0 & 0 \end{pmatrix}\begin{pmatrix} 0 & 0 & 0 \\ 1 & 0 & 0 \\ 0 & 0 & 0 \end{pmatrix} + \begin{pmatrix} 0 & 0 & 0 \\ 1 & 0 & 0 \\ 0 & 0 & 0 \end{pmatrix}\begin{pmatrix} 0 & 1 & 0 \\ 0 & 0 & 0 \\ 0 & 0 & 0 \end{pmatrix}\right] =$$

$$= \frac{-\sqrt{2}}{f}\partial_\mu(\pi^+)\Sigma^- \left[\begin{pmatrix} 1 & 0 & 0 \\ 0 & 1 & 0 \\ 0 & 0 & 0 \end{pmatrix}\right] \tag{C3}$$

$$[u_\mu, B] = \frac{-\sqrt{2}}{f}\partial_\mu(\pi^+)\Sigma^- \left[\begin{pmatrix} 0 & 1 & 0 \\ 0 & 0 & 0 \\ 0 & 0 & 0 \end{pmatrix}\begin{pmatrix} 0 & 0 & 0 \\ 1 & 0 & 0 \\ 0 & 0 & 0 \end{pmatrix} - \begin{pmatrix} 0 & 0 & 0 \\ 1 & 0 & 0 \\ 0 & 0 & 0 \end{pmatrix}\begin{pmatrix} 0 & 1 & 0 \\ 0 & 0 & 0 \\ 0 & 0 & 0 \end{pmatrix}\right] =$$

$$= \frac{-\sqrt{2}}{f}\partial_\mu(\pi^+)\Sigma^- \left[\begin{pmatrix} 1 & 0 & 0 \\ 0 & -1 & 0 \\ 0 & 0 & 0 \end{pmatrix}\right]. \tag{C4}$$

Both traces may now be evaluated, taking in account that γ_5 and γ^μ are in Dirac space, which allows us to take this terms out of the trace:

$$\frac{D}{2}\text{Tr}[\bar{B}\gamma^\mu\gamma_5\{u_\mu, B\}] = \frac{D}{2}\gamma^\mu\gamma_5\text{Tr}[\bar{B}\{u_\mu, B\}] =$$

$$= \frac{D}{2}\gamma^\mu\gamma_5\left(\frac{-\sqrt{2}}{f}\partial_\mu(\pi^+)\Sigma^-(\frac{1}{\sqrt{2}}\bar{\Sigma}^0)\right)\text{Tr}\begin{pmatrix} 1 & 0 & 0 \\ 0 & -1 & 0 \\ 0 & 0 & 0 \end{pmatrix} = 0 \tag{C5}$$

$$\frac{F}{2}\text{Tr}[\bar{B}\gamma^\mu\gamma_5[u_\mu, B]] = \frac{D}{2}\gamma^\mu\gamma_5\text{Tr}[\bar{B}[u_\mu, B]] =$$

$$= \frac{D}{2}\gamma^\mu\gamma_5 \left(\frac{-\sqrt{2}}{f}\partial_\mu(\pi^+)\Sigma^-(\frac{1}{\sqrt{2}}\bar{\Sigma}^0)\right)\text{Tr}\begin{pmatrix} 1 & 0 & 0 \\ 0 & 1 & 0 \\ 0 & 0 & 0 \end{pmatrix} = -\frac{D}{2f}\gamma^\mu\gamma_5\partial_\mu(\pi^+)\Sigma^-(\bar{\Sigma}^0). \tag{C6}$$

2. Weak PV example: the $\Sigma^+\pi^- \to n$ vertex

Analogously as the strong coupling constants, the computations for the PV weak values is pretty straightforward. For the weak case, though, all the Lagrangian terms are used. In this example it is computed the vertex $\Sigma^-\pi^+ \to n$ starting, once more, by computing both the commutator and anticommutator from:

$$\mathcal{L}^{PV} = G_F m_\pi^2 \sqrt{2}f_\pi \left(h_D\text{Tr}[\bar{B}\{\xi^\dagger h\xi, B\}] + h_F\text{Tr}[\bar{B}[\xi^\dagger h\xi, B]]\right), \tag{C7}$$

with the particular values for B, $\bar{B}$ and ϕ:

$$B = \begin{pmatrix} 0 & 0 & 0 \\ \Sigma^- & 0 & 0 \\ 0 & 0 & 0 \end{pmatrix} \quad \bar{B} = \begin{pmatrix} 0 & 0 & 0 \\ 0 & 0 & 0 \\ 0 & \bar{n} & 0 \end{pmatrix} \quad \phi = \begin{pmatrix} 0 & \pi^+ & 0 \\ 0 & 0 & 0 \\ 0 & 0 & 0 \end{pmatrix}. \tag{C8}$$

The value for $\xi^\dagger h\xi$ is:

$$\xi^\dagger h\xi = h + [h, \phi]\frac{i}{\sqrt{2}f} = \begin{pmatrix} 0 & 0 & 0 \\ 0 & 0 & 1 \\ 0 & 0 & 0 \end{pmatrix} + \frac{i}{\sqrt{2}f}\left[\begin{pmatrix} 0 & 0 & 0 \\ 0 & 0 & 0 \\ 0 & 0 & 0 \end{pmatrix} - \begin{pmatrix} 0 & 0 & \pi^+ \\ 0 & 0 & 0 \\ 0 & 0 & 0 \end{pmatrix}\right] = \begin{pmatrix} 0 & 0 & -i\frac{\pi^+}{\sqrt{2}f} \\ 0 & 0 & 1 \\ 0 & 0 & 0 \end{pmatrix}. \tag{C9}$$

This result is used now to get the commutator and anti-commutator:

$$[\xi^\dagger h\xi, B] = i\frac{\pi^+}{\sqrt{2}f}\Sigma^-\begin{pmatrix} 0 & 0 & 0 \\ 0 & 0 & 1 \\ 0 & 0 & 0 \end{pmatrix} \tag{C10}$$

$$\{\xi^\dagger h\xi, B\} = -i\frac{\pi^+}{\sqrt{2}f}\Sigma^-\begin{pmatrix} 0 & 0 & 0 \\ 0 & 0 & 1 \\ 0 & 0 & 0 \end{pmatrix}. \tag{C11}$$

The last step is computing the trace of these last steps times the antibaryon matrix $\bar{B}$:

$$G_F m_\pi^2\sqrt{2}f_\pi[-h_D + h_F]i\frac{\pi^+}{\sqrt{2}f}\text{Tr}\begin{pmatrix} 0 & 0 & 0 \\ 0 & 0 & 0 \\ 0 & 0 & \bar{n} \end{pmatrix} = -G_F m_\pi^2 f_\pi[h_D - h_F]i\frac{\pi^+}{f}. \tag{C12}$$

3. Weak PC example: the $\Sigma^+\pi^- \to n$ vertex

To exemplify one of the PC weak coupling constants using the pole model, we are going to use the example depicted before in Figure (5). This is the case for the transition $\Sigma^+\pi^- \to n$. The Eq. (42) is explicitly written again:

$$g_{\Sigma^+\Lambda\pi^-}\frac{1}{m_n - m_\Lambda}A_{\Lambda n} + g_{\Sigma^+\Sigma^0\pi^-}\frac{1}{m_n - m_{\Sigma^0}}A_{\Sigma^0 n} + g_{pn\pi^-}\frac{1}{m_{\Sigma^+} - m_p}A_{\Sigma p}. \qquad (C13)$$

The pole model, as we mentioned before, is based in shifting the strong vertex along the baryonic line. Each appearing diagram will have its corresponding term.

As if they were separate vertices, we take the corresponding strong baryon-baryon-meson coupling constant, which are also written down in Table IV, and we divided by the difference of masses we get, towards the strong vertex. This term must be multiplied by the corresponding $A_{B_1 B_2}$ [10][12] constant, with B_1 and B_2 the initial and final baryons of the new weak vertex.

The expressions obtained with this model are shown in Table VI.

4. Total coupling constants contribution.

Here is an example of how strong and weak coupling constants are finally integrated. The computations here are given for the $\Sigma^-\Sigma^+ \xrightarrow{\pi^-} n\Lambda$ transition:

$$< \frac{1}{2}t_{Nf}, T_Y t_Y|\vec{T}_1\vec{T}_2|\frac{3}{2}t, T_2 t_2 >< \frac{3}{2}t|1-1\frac{1}{2}-\frac{1}{2} >=$$

$$= \sum_\mu (-1)^\mu < \frac{1}{2}t_{Nf}|\vec{T}_1|\frac{3}{2}t >< T_Y t_Y|\vec{T}_2|T_2 t_2 >< \frac{3}{2}t|1-1\frac{1}{2}-\frac{1}{2} >=$$

$$= \sum_\mu (-1)^\mu < \frac{1}{2}-\frac{1}{2}|\vec{T}_1|\frac{3}{2}-\frac{3}{2} >< 00|\vec{T}_2|11 >< \frac{3}{2}\frac{-}{3}2|1-1\frac{1}{2}-\frac{1}{2} >= \qquad (C14)$$

$$= (-1)\left[\frac{< \frac{3}{2}-\frac{3}{2}1\mu|\frac{1}{2}-\frac{1}{2} >< \frac{1}{2}|\vec{T}_1|\frac{3}{2} >}{\sqrt{2}}\right](-1) = -1.$$

It is necessary to mention why there is a null term in the product of coupling constants for $\Sigma^0\Sigma^0 \xrightarrow{\pi^0} n\Sigma^0$. The responsible is the following term:

$$< T_Y t_Y|\vec{T}_2|T_2 t_2 >=< 10|\vec{T}_2|10 >= 0, \qquad (C15)$$

which leads to a zero result.

References

[1] E. Oset, P. Fernandez de Cordoba, L. L. Salcedo, and R. Brockmann. Decay Modes of Σ and Λ Hypernuclei. *Phys. Rept.*, 188:79, 1990.

[2] Isaac Vidaña. Hyperons: the strange ingredients of the nuclear equation of state. *Proc. Roy. Soc. Lond.*, A474:0145, 2018.

[3] W. M. Alberico and G. Garbarino. Weak decay of Lambda hypernuclei. *Phys. Rept.*, 369:1–109, 2002.

[4] A. Parreno, A. Ramos, C. Bennhold, and Kim Maltman. Violation of the Delta(I) = 1/2 rule in the non-mesonic weak decay of hypernuclei. *Phys. Lett.*, B435:1–8, 1998.

[5] J. K. Ahn et al. Double-Λ hypernuclei observed in a hybrid emulsion experiment. *Phys. Rev.*, C88(1):014003, 2013.

[6] K. Nakazawa. Lambda Lambda interaction indicated by 'Lambpha' (Lambda Lambda)He-6 double hypernucleus). *AIP Conf. Proc.*, 603(1):463–466, 2001.

[7] Kazuma Nakazawa et al. Study of Double-strangeness Nuclear Systems with Nuclear Emulsion. *Phys. Procedia*, 80:69–73, 2015.

[8] A. Parreno, A. Ramos, and C. Bennhold. Novel weak decays in doubly strange systems. *Phys. Rev.*, C65:015205, 2002.

[9] Jordi Maneu, Assumpta Parreõ, and Àngels Ramos. Effects of $\Lambda\Lambda - \Xi N$ mixing in the decay of $S = -2$ hypernuclei. *Phys. Rev.*, C98(2):025208, 2018.

[10] Jordi Maneu. *Decay of Doubly Strange nuclei.* PhD thesis, Universitat de Barcelona, 12 2019.

[11] M. Tanabashi et al. Review of particle physics. *Phys. Rev. D*, 98:030001, Aug 2018.

[12] Assum Parreño. *The nonmesonic decay of hypernuclei.* PhD thesis, Universitat de Barcelona, 5 1997.

[13] Y. Goto et al. Polarized parton distribution functions in the nucleon. *Phys. Rev.*, D62:034017, 2000.

[14] Ghil-Seok Yang and Hyun-Chul Kim. Meson–baryon coupling constants of the SU(3) baryons with flavor SU(3) symmetry breaking. *Phys. Lett.*, B785:434–440, 2018.

[15] J.F. Donoghue, E. Golowich, and B.R. Holstein. *Dynamics of the Standard Model.* Cambridge Monographs on Particle Physics, Nuclear Physics and Cosmology. Cambridge University Press, 1994.

[16] Roxanne Patricia Springer. Heavy baryon chiral perturbation theory and the weak nonleptonic p wave decays of the baryon octet. *Phys. Lett.*, B461:167–174, 1999.

[17] A. R. Edmonds. *Angular Momentum in Quantum Mechanics.* Princeton University Press, 1957.

[18] Jordi Maneu. Private Communication.